

An Estimate of Twist-Four Contributions at Small x_B and Low Q^2

Jochen Bartels and Claas Bontus

*II. Institut für Theoretische Physik, Universität Hamburg,
Luruper Chaussee 149, D-22761 Hamburg¹*

We present a first study of gluonic twist-four corrections to the deep inelastic structure function F_2 at small x and small Q^2 . The calculations are based upon the double logarithmic approximation of the coupled twist-four evolution equations of the gluonic twist-four operators that are expected to be dominant at small x . We first review the analytical results which are presently available and define the framework of our calculation. In the second part we discuss the connection with DIS diffractive dissociation which can be used to estimate the size of some of the twist-four corrections. In the final part we show, for three different choices of the input distributions, the relative magnitude of the leading-twist and the twist-four contributions.

Supported by the TMR Network “QCD and Deep Structure of Elementary Particles”. One of us (C.B.) is supported by *Graduiertenkolleg Theoretische Elementarteilchenphysik*.

¹email: bartels@x4u2.desy.de claas.bontus@desy.de

1 Introduction

The observation that the rise of the deep inelastic structure function F_2 at small x starts already at surprisingly low values of Q^2 , has stimulated attempts to use the DGLAP evolution equations in the low Q^2 kinematical regime [1–3], where previously – i.e. before the advent of HERA – perturbative QCD had not been expected to be applicable. As a general result of these studies, with a suitable choice of initial conditions (in particular: not rising at small x) it is possible to describe, within the framework of the leading-twist, next-to-leading-order QCD evolution equations, the Q^2 -evolution of the structure functions down to rather low Q^2 values. However, recently [4] evidence has been given that a rather sharp transition away from this DGLAP evolution occurs between $3 \text{ GeV}^2 < Q^2 < 8 \text{ GeV}^2$, $10^{-4} < x < 10^{-3}$.

The apparent success of DGLAP in the low Q^2 region, however, does not provide much help for answering the question of how the transition from the perturbative parton picture into the non-perturbative hadronic region at $Q^2 = 0$ works. Most naively, one expects the breakdown of perturbative QCD to be accompanied by the growth of non-leading perturbative terms. For deep inelastic scattering, the expansion parameters are powers of the strong coupling constant α_s and powers of m^2/Q^2 (with m denoting some hadronic scale) which define the twist expansion. Whereas the former expansion has already received some attention (e.g. the question of resummation in the anomalous dimension for small x [5]), the rôle of non-leading twist at small x so far has not yet been addressed. In particular, if at low Q^2 the transition between the parton picture and Regge physics results from an interplay of leading-twist and higher-twist corrections, one should expect to see the presence of a negative twist-four term already *slightly above* the transition. The results of [4] indicate that twist-four might be present even at not so small values of Q^2 . If this is the case, existing leading-twist parametrizations in the low Q^2 -region need to be re-examined. If, on the other hand, higher-twist really remains small down to unexpected low values of Q^2 , one should look for an explanation of this phenomenon. In any case, a closer investigation of the rôle of higher-twist in the small x , low Q^2 -region is quite important.

Twist-four operators are known [6] to have their own evolution equations. For the small x domain, gluon operators are expected to be the dominant ones. Whereas fermionic twist-four operators have been investigated in some detail, very little is known about the gluonic ones. Following the arguments of [7] we expect that twist-four gluonic contributions are obtained by investigating the Q^2 -dependence of QCD diagrams with two, three, or four gluons in the t -channel. Explicit calculations of these diagrams have been done only for the small x behavior of gluonic scattering amplitudes: the BFKL [8] (ladder) amplitude, from which one obtains the high energy behavior of the elastic scattering of a virtual photon on a gluon, and diffractive deep inelastic scattering in the triple Regge region [9], which allows to extract contributions with three and four gluons in the t -channel. Expanding these amplitudes in inverse powers of Q^2 we expect to reproduce the Q^2 evolution equations for twist-two and twist-four in the double leading log approximation (DLA): leading logarithmic in both $\ln Q^2$ and $\ln 1/x$. A complete leading order calculation of the Q^2 -evolution equations of the twist-four gluon operators is missing, and it is very important that this task will be addressed. In this paper we will adopt the viewpoint that the combined limit: $x \rightarrow 0$, $Q^2 \rightarrow \infty$ of diagrams with two, three, or four gluons in the t -channel provides the DLA for the twist-four gluon operators.

A numerical analysis of twist-four corrections to, say, F_2 follows the same sequence of steps as the usual twist-two strategy: for an input scale Q_0^2 one has to choose an initial distribution (with a

certain number of free parameters), and by application of evolution equations one gets values of the structure functions for larger Q^2 . Since the number of twist-four operators that mix under renormalization will, in general, be larger than in the twist-two case, the number of free parameters in such an analysis will be large, and a reliable combined analysis of twist-two and twist-four terms looks extremely difficult. It might, therefore, be helpful to include information on specific final states, which are known to belong to higher-twist. At present the most promising candidate are diffractive final states, in particular the diffractive production of vector mesons from longitudinal photons: this process has been shown to be calculable within perturbative QCD [10–13]. It belongs to higher-twist, and the measured cross section is substantial (about 20% of the total diffractive cross section). Another potential source of information are diffractive final states with hard jets.

In this paper we perform a first numerical estimate of gluonic twist-four corrections at small x and low Q^2 . For this we make use of the currently available elements of the twist-four evolution equations. In our scheme we, first, review the existing small x calculations of gluonic scattering amplitudes, and extract from them the relevant pieces of the Q^2 evolution. The currently existing calculations do not allow to go beyond DLA. Generally we are dealing with gluonic amplitudes which couple to the photon through a fermion-loop. As a first general result we find that, for a systematic study of twist-four, we have to consider both the transverse and the longitudinal polarization of the photon. The reason for this is the fact that in the fermion-loop the twist-four contribution of the transverse photon loses one power of $\ln Q^2$, whereas the longitudinal photon does not. This is quite opposite to the leading-twist case where the transverse photon results in a logarithm, and the longitudinal one does not. Unfortunately, in DLA this result forces us to compare contributions of different order in α_s : in order to make a legitimate comparison between the twist-four transverse and longitudinal contributions, we should know the longitudinal one up to the (in the sense of DLA) next-to-leading terms. We, therefore, restrict ourselves to ratios of twist-four corrections to DLA leading-twist results. A second general result of our investigation is the sign structure of the different higher-twist terms. Both for the longitudinal and for the transverse twist-four contributions we shall argue that there are four different pieces that have to be taken into account, and they come with alternating signs. The total twist-four contribution, therefore, depends crucially on the magnitude of each individual term, i.e. the size of the initial condition.

The second purpose of this paper is the search for a practical procedure for estimating the higher-twist contributions. We propose to use experimental data of DIS diffractive final states. It is, therefore, necessary to first investigate the rôle of higher-twist in diffractive dissociation and to analyse the connection with the inclusive structure functions. In the second part of this paper we, therefore, review diffractive dissociation, with particular emphasis on higher-twist. For the determination of free parameters in our numerical analysis we will make use only of longitudinal quark-antiquark production; in order to understand the origin of the different signs, however, we have to analyse also other diffractive final states. Contact with the corrections to the structure functions is made through the AGK cutting rules [14]. We find that, in contrast to the naive expectation, we cannot simply use the diffractive cross section to determine the higher-twist corrections to F_2 . There still remains an unknown piece in the initial conditions which we presently cannot determine. Our central result on the AGK rules is contained in eqn. (3.21).

In the final part of this paper we present results of a numerical analysis. We write

$$F_i(x, Q^2) = F_i^{\tau=2} + \Delta F_i, \quad i = t, \ell \quad (1.1)$$

and compare the different pieces. The twist-four correction ΔF_i (both for $i = t$ and $i = \ell$) consists

of four pieces (cf. (2.46)), and we will present numerical results for them, all normalized to $F_t^{\tau=2}$. Because of the uncertainty in the initial conditions, we consider three different choices, two with flat (in x) input distributions, and one with a rising x -distribution. As one of our main results for the first two scenarios, we find, despite the strong cancellations among the different twist-four contributions, that the total twist-four contribution is not small at $Q^2 = 1 \text{ GeV}^2$ (between 15% and 130%). It is negative and mainly due to the transverse photon. Unfortunately, the severe limitation due to the DLA, together with the uncertainties of the initial conditions prevents us from obtaining a more precise estimate.

The outline of this paper is as follows. In section 2 we give an overview of the higher-twist results which are presently available, and of the formulae that we are using in our analysis. For a systematic study of twist-four at small x we find that it is necessary to consider contributions of amplitudes with two, three and four gluons in the t -channel. We discuss these contributions in several subsections and outline how we handle the problem of running α_s . Next (section 3), we analyse the rôle of higher-twist in DIS diffraction and we study the connection with the deep inelastic structure function. Finally, in section 4 we describe the numerical calculations and present and discuss our results.

2 Higher-Twist at small x

We begin with a brief summary of the present theoretical status of the evolution of higher-twist operators. A systematic classification of twist-four operators can, in principle, be obtained using the arguments of R. K. Ellis et.al. [7]. However, in [7] (and in several other studies of higher-twist operators [15]) only fermionic twist-four operators have been considered. At small x , on the other hand, it is the pure gluonic operators that are expected to dominate, and a systematic discussion of twist-four gluon operators is missing. General dimensional arguments lead to the following operators. First, there are the four-gluon operators:

$$\begin{aligned} & \text{Tr } F^{\mu_1 \alpha} \dots F^{\mu_i}_{\alpha} \dots F^{\mu_j \beta} \dots F^{\mu_n}_{\beta} \\ & \text{Tr } F^{\mu_1 \alpha} \dots F^{\mu_i \beta} \dots F^{\mu_j}_{\alpha} \dots F^{\mu_n}_{\beta} \\ & \text{Tr } F^{\mu_1 \alpha} \dots F^{\mu_i \beta} \dots F^{\mu_j}_{\beta} \dots F^{\mu_n}_{\alpha} \end{aligned} \quad (2.1)$$

(here $1 < i, j < n$, and the dots denote products of covariant derivatives). In [6] these operators have been named “quasipartonic”, and a general discussion of their evolution has been given. In particular, it has been shown that to leading order only two-body interaction kernels are needed. They are the non-forward generalizations of the AP splitting functions. An analysis of the small x evolution equations in DLA can be found in [16]. In addition to the quasipartonic operators (2.1), there exists another gluonic twist-four operator which is contained in the BFKL equation:

$$\text{Tr } F^{\mu_1 \alpha} D^{\mu_2} \dots D^{\mu_{n-1}} F^{\mu_n}_{\alpha} g^{\perp}_{\mu_i \mu_j} + \text{Perm} . \quad (2.2)$$

In DLA the anomalous dimension of this operator can be derived from the BFKL equation; the recently derived [17] second order corrections to the BFKL kernel allow to go beyond DLA. In general, the twist-four operators (2.1) and (2.2) should mix, i.e. there should be off-diagonal elements in the anomalous dimension matrix. These off-diagonal elements are known in DLA-accuracy [16].

In the discussion below we shall see that the operators (2.1) are the most interesting ones at small x : they result in contributions which rise stronger at small x than the contributions of the leading-twist gluon operator. Therefore, at sufficiently small x , this operator will catch up with the leading-twist contributions, despite its $1/Q^2$ suppression. On the other hand, power counting in α_s will show that (2.1) is suppressed compared to (2.2): again, because of the strong small x rise in (2.1), (2.1) will eventually dominate over (2.2). The α_s -suppression of (2.1) will, however, force us to consider higher order corrections to (2.2).

In the following we shall list the presently available results for the operators (2.1) and (2.2). They do not allow us to go beyond the DLA approximation. It remains a major theoretical effort that has to be made in order to calculate the full leading order evolution kernels of the gluonic operators.

2.1 The Two-Gluon Operator

As we have said before, the DLA approximation of the anomalous dimension of the twist-four two-gluon operator can be obtained from the BFKL equation. Let $D_2^i(x, Q_0^2/Q^2)$ ($i = t, \ell$) denote the imaginary part of the scattering amplitude of the photon (virtuality Q^2) off the gluon (virtuality Q_0^2). It is convenient to write this amplitude as a double Mellin-transformation

$$D_2^i(x, Q_0^2/Q^2) = \int \frac{d\omega}{2\pi i} x^{-\omega} \int_{-1/2-i\infty}^{-1/2+i\infty} \frac{d\nu}{2\pi i} \left(\frac{Q_0^2}{Q^2}\right)^{-\nu} D_2^i(\omega, \nu). \quad (2.3)$$

In the BFKL approximation, the amplitude $D_2^i(\omega, \nu)$ can be written as

$$D_2^i(\omega, \nu) = D_{2,0}^i(\nu) \frac{1}{\omega - \chi(\nu)}, \quad (2.4)$$

where $D_{2,0}^i$ denotes the quark-loop at the upper end of the gluon ladder (fig. 1a), and the BFKL characteristic function has the form

$$\chi(\nu) = \frac{N_c \alpha_s}{\pi} [2\psi(1) - \psi(\nu + 1) - \psi(-\nu)]. \quad (2.5)$$

It has poles at integer values of ν , and the anomalous dimensions of the leading-twist two-gluon operator and the twist-four two-gluon operator are obtained by solving the equation

$$0 = \omega - \chi(\nu) \quad (2.6)$$

near the poles at $\nu = -1$ and $\nu = -2$, resp.:

$$\gamma^{\tau=2}(\omega) = \frac{N_c}{\pi\omega} \alpha_s + \mathcal{O}\left(\left(\frac{\alpha_s}{\omega}\right)^4\right) \quad (2.7)$$

$$\gamma^{\tau=4}(\omega) = \frac{N_c}{\pi\omega} \alpha_s - 2 \left(\frac{N_c \alpha_s}{\pi\omega}\right)^2 + \mathcal{O}\left(\left(\frac{\alpha_s}{\omega}\right)^3\right). \quad (2.8)$$

Using the recently published NLO calculations [17] it is possible to derive the singular part of the NLO corrections to the anomalous dimensions, i.e. corrections of the form $\alpha_s^2 \frac{\text{const.}}{\omega}$.

n	a_n^ℓ	b_n^ℓ	a_n^t	b_n^t
1	$\frac{2}{3}$	0	$\frac{14}{9}$	$\frac{4}{3}$
2	$-\frac{94}{225}$	$-\frac{4}{15}$	$\frac{2}{3}$	0

TABLE 1: Twist-expansion coefficients of $D_{2,0}$ for leading- and next-to-leading twist.

The coefficient functions are derived from the quark-loop $D_{2,0}^i(\omega, \nu)$. We begin with the result for the transverse photon [9, 18]:

$$\frac{1}{\omega} D_{2,0}^t(\omega, \nu) = \frac{1}{\omega} \sum_f e_f^2 \frac{\sqrt{8}}{2\pi} \alpha_s \frac{\pi^2}{4} \frac{(\nu-1)(\nu+2)}{(\nu-\frac{1}{2})(\nu+\frac{1}{2})(\nu+\frac{3}{2})} \frac{\sin[\pi(\nu+\frac{1}{2})]}{\cos^2[\pi(\nu+\frac{1}{2})]}. \quad (2.9)$$

Similarly, for the longitudinal photon one has:

$$\frac{1}{\omega} D_{2,0}^\ell(\omega, \nu) = \frac{1}{\omega} \sum_f e_f^2 \frac{\sqrt{8}}{2\pi} \alpha_s \frac{\pi^2}{4} \frac{\nu(\nu+1)}{(\nu-\frac{1}{2})(\nu+\frac{1}{2})(\nu+\frac{3}{2})} \frac{\sin[\pi(\nu+\frac{1}{2})]}{\cos^2[\pi(\nu+\frac{1}{2})]}. \quad (2.10)$$

By expanding eqns. (2.9) and (2.10) in Laurent-series,

$$D_{2,0}^{t,\ell}(\omega, \nu) = \sum_f e_f^2 \frac{\sqrt{8}}{2\pi} \alpha_s \sum_{n=-\infty}^{\infty} \left(\frac{b_n^{t,\ell}}{(\nu+n)^2} + \frac{a_n^{t,\ell}}{\nu+n} \right), \quad (2.11)$$

and considering the residues at negative integer values of ν we obtain the twist expansion in powers of Q_0^2/Q^2 . The coefficients a_n and b_n for leading- and next-to-leading twist are listed in table 1. Since the double poles in the b_n -terms correspond to logarithms of Q^2 while the single poles in the a_n -terms correspond to constants, we recognize with the help of table 1 that, for leading-twist, the longitudinal contribution is sub-leading at large Q^2 (compared to the transverse cross section). For twist-four we have the opposite situation: the longitudinal contribution has the $\ln Q^2/Q_0^2$, whereas the transverse cross section is suppressed. Moreover, we note the sign structure of the coefficients in table 1: the twist-four contribution of the longitudinal cross section comes with a negative sign.

For our twist-four analysis we perform the computations in DLA and, therefore, consider only amplitudes proportional to b_2^ℓ and a_2^t for the longitudinal and transverse contributions, respectively. Taking into account the evolution in Q^2 , we get, for each rung, a factor $\gamma_2/\omega(\nu+2)$, where²

$$\gamma_2 \equiv \frac{N_c \alpha_s}{\pi}. \quad (2.12)$$

Performing the ν -integration we end up with

$$D_2^t(\omega, Q_0^2/Q^2)^{\tau=4} = a_2^t \sum_f e_f^2 \frac{\sqrt{8}}{2\pi} \alpha_s \left(\frac{Q_0^2}{Q^2} \right)^2 \frac{1}{\omega} \exp\left(\frac{\gamma_2}{\omega} \ln(Q^2/Q_0^2)\right), \quad a_2^t = \frac{2}{5} \quad (2.13)$$

for the transverse amplitude, and

$$D_2^\ell(\omega, Q_0^2/Q^2)^{\tau=4} = b_2^\ell \sum_f e_f^2 \frac{\sqrt{8}}{2\pi} \frac{\alpha_s}{\gamma_2} \left(\frac{Q_0^2}{Q^2} \right)^2 \left[\exp\left(\frac{\gamma_2}{\omega} \ln(Q^2/Q_0^2)\right) - 1 \right], \quad b_2^\ell = -\frac{4}{15} \quad (2.14)$$

²Within our conventions the singular part of the gluon anomalous dimension is given by γ_2/ω and not by γ_2 itself.

for the longitudinal one. As stated before, the longitudinal amplitude has an extra factor $\ln Q^2/Q_0^2$, in comparison with the transverse case: in the DLA approximation, therefore, we have to be careful when comparing the transverse amplitude with the longitudinal one. However, the extra logarithm only emphasises the dominance of the longitudinal amplitude at large Q^2 . In the low Q^2 region, there is no reason why the (twist-four) part of the transverse cross section should be smaller than the longitudinal one. We will, therefore, be slightly inconsistent with the counting of ‘leading’ and ‘sub-leading’.

Finally, we note the connection between the amplitudes $D_2^{t,\ell}$ and the twist-four corrections to the structure functions:

$$\Delta F_{t,\ell}^{(2)}(x, Q^2) = \frac{1}{2\sqrt{8}} \frac{Q^2}{Q_0^2} \int \frac{d\omega}{2\pi i} x^{-\omega} \int_{-1/2-i\infty}^{-1/2+i\infty} \frac{d\nu}{2\pi i} \left(\frac{Q_0^2}{Q^2}\right)^{-\nu} D_2^{t,\ell}(\omega, \nu) \varphi_2(\omega, \nu)^{\tau=4}, \quad (2.15)$$

where the superscript ‘2’ on the l.h.s. refers to the ‘2-gluon’ ladder. In the subsequent sections we will add further terms to ΔF_i . Within our representations the twist-four part is obtained by evaluating the residue at $\nu = -2$ (from $\nu = -1$ we get the leading-twist term). $\varphi_2(\omega, \nu)$ denotes the initial condition: in the context of the BFKL equation (which is an evolution equation in $y = \ln 1/x$) φ_2 would define, at fixed x_0 , the distribution in Q^2 . However, in our DLA approximation, where the BFKL equation coincides with the small x limit of the DGLAP evolution equation, φ_2 denotes, at fixed scale Q_0^2 , the initial distribution in x . In the (ω, ν) -representation, φ_2 depends upon both ν and ω and contains both leading-twist and higher-twist: the ω singularity structure near $\nu = -1$ defines the x -shape of the leading-twist initial distribution of the gluon structure function, and the behavior near $\nu = -2$ determines the input to the twist-four correction. As usual, both input distributions have to be modelled and cannot be computed within pQCD. In the following, unless stated differently, we will use φ_2 to denote the leading-twist initial distribution.

Our discussion below will show that the situation with the two-gluon amplitude, in fact, is more complicated. In particular, we shall argue that the reggeization of the gluon provides extra contributions to the two-gluon operator. Namely, in the next subsection we will turn to a discussion of the four-gluon operators (2.1). To lowest order in α_s , it involves diagrams in which four gluons are exchanged between the quark-loop and the target proton (fig. 2). These diagrams are suppressed by one factor α_s compared to the two-gluon operator (2.2). At small x , however, this suppression is compensated by the stronger rise of the four-gluon operator contributions. When higher order gluon diagrams are included, it will turn out that, at small x , the sum of all these diagrams has to be split up into two separate classes. The first one corresponds to the expected four-gluon operator (which, however, mixes with the two-gluon operator (2.2)). For this piece, the α_s -suppression (relative to the twist-four two-gluon operator) is compensated by the stronger rise at small x . However, in addition to this contribution to the four-gluon operator there is a second set which results from the reggeization of the gluon. This contribution has the same form of gluon ladders as the BFKL equation, except that at the lower end the reggeizing gluon lines split up into two or more gluon propagators (fig. 4). Starting from the lower end, the four-gluon state immediately turns into a state of two reggeized gluons. It, therefore, has the same Q^2 -dependence as the BFKL amplitude, but counting powers of α_s , it is of higher order than the BFKL ladder discussed above. The lowest order diagram is the four-gluon diagram in fig. 2, but in higher order it turns into a (higher order) contribution to the initial distribution of the two-gluon operator. We will show that this contribution can be related to the measured diffractive cross section. After the discussion in the next

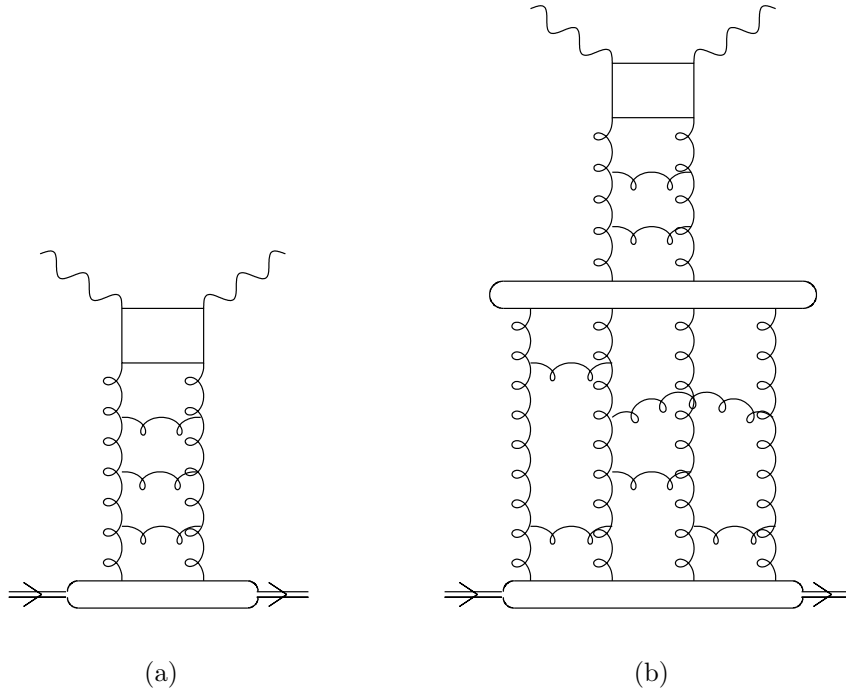


FIG. 1: (a) The two-gluon amplitude and (b) D_4^I , the part of the four-gluon amplitude which is *irreducible* with respect of reggeization.

subsection we, therefore, will, once more, return to the two-gluon operator (2.2) and add two more separate contributions.

To summarize the main results of this subsection, starting from the BFKL amplitude we have collected the known results on the twist-four two-gluon operator (2.2). Rather than writing the BFKL amplitude as an evolution equation we have used the closed expression in the (ω, ν) -representation. Presently, only expressions within the DLA are completely available. In order to go beyond the DLA it will be necessary to perform a more complete calculation. For the anomalous dimension in (2.8), the next-to-leading order can be extracted from the recent results of the second order BFKL kernel [17]. For the coefficient functions ((2.9), (2.10)) such a calculation has not yet been performed.

2.2 The Four-Gluon Operator

While the contributions of the two-gluon twist-four operator (2.2) could be derived with the help of the BFKL equation, the four-gluon operators (2.1) require a separate study. The simplest diagrams are shown in fig. 2. In the limit of small x , these diagrams (together with higher order corrections) have been investigated in [9, 16], and we simply summarize the results and relate them to the operators (2.1) and (2.2).

In the investigation of [9, 16], the starting point was the triple Regge limit of a six-point amplitude; from this an amplitude D_4 was defined which describes the coupling of four t -channel gluons to two virtual photons. We recall only those results which are relevant for our analysis. The four-gluon

amplitude D_4 satisfies an integral equation which we illustrate with the help of fig. 3. As one main result of ref. [9], it was shown that D_4 should be written as a sum of two pieces, the *reggeizing* terms D_4^R , which consist of terms proportional D_2 (eqn. (2.41) below), and terms which are *irreducible* with respect of reggeization D_4^I :

$$D_4 = D_4^R + D_4^I. \quad (2.16)$$

The two terms on the r.h.s. can also be distinguished by their symmetry properties: whereas D_4^I is totally symmetric under permutation of the outgoing gluons, the term D_4^R has mixed symmetry properties. In the following we shall discuss these contributions in some detail. In particular, we shall interpret them in terms of the operators (2.1) and (2.2). In order to avoid a too complicated notation, we will from now on suppress the reference to the photon polarization.

We choose our conventions such that the connection with the cross section σ_{γ^*p} is as follows:

$$\sigma_{\gamma^*p} = -\frac{4\pi^2\alpha_{em}}{Q^2} \frac{1}{128\pi^2} \int \frac{d\omega}{2\pi i} \left(\frac{1}{x}\right)^\omega \int \frac{d\nu}{2\pi i} \left(\frac{Q_0^2}{Q^2}\right)^{-\nu-1} D_4^{abcd} \varphi_4^{abcd}. \quad (2.17)$$

In the following we will describe this formula in more detail. In particular, the overall minus sign in front will be derived with the help of the AGK rules [14].

We begin with the *irreducible* part. Since D_4^R has a particularly simple form (fig. 4 and eqn. (2.41) below), we simply subtract it on both sides of the equation in fig. 3 and make use of the integral equation for D_2 . Regrouping the terms on the r.h.s. of fig. 3, one arrives at the following integral equation:

$$\omega D_4^{I;abcd}(\mathbf{k}_1, \mathbf{k}_2, \mathbf{k}_3, \mathbf{k}_4) = \left[D_2 \otimes V^{abcd} + D_4^{I;abcd} \otimes \sum (K_{2 \rightarrow 2} + \alpha - 1) \right] (\mathbf{k}_1, \mathbf{k}_2, \mathbf{k}_3, \mathbf{k}_4). \quad (2.18)$$

Here $\mathbf{k}_1, \dots, \mathbf{k}_4$ are the transverse components (in the Sudakov decomposition) of the momenta of the four gluons at the lower end in fig. 1b, and a, b, c, d are the corresponding color labels. $K_{2 \rightarrow 2}$ and α are the common BFKL kernel and the gluon trajectory function, and the sum has to be taken over all possible pairs of gluons. V represents the transition vertex from $2 \rightarrow 4$ gluons (fig. 1b),

$$\begin{aligned} V^{abcd} = \frac{g^2}{12\sqrt{2}} \Big\{ & \delta^{ab}\delta^{cd} [G(\mathbf{k}_1, \mathbf{k}_3) + G(\mathbf{k}_2, \mathbf{k}_3) + G(\mathbf{k}_1, \mathbf{k}_4) + G(\mathbf{k}_2, \mathbf{k}_4) - \\ & - G(\mathbf{k}_1, \mathbf{k}_3 + \mathbf{k}_4) - G(\mathbf{k}_2, \mathbf{k}_3 + \mathbf{k}_4) - G(\mathbf{k}_3, \mathbf{k}_1 + \mathbf{k}_2) - \\ & - G(\mathbf{k}_4, \mathbf{k}_1 + \mathbf{k}_2) + G(\mathbf{k}_1 + \mathbf{k}_2, \mathbf{k}_3 + \mathbf{k}_4)] + \\ & + \delta^{ac}\delta^{bd} [G(\mathbf{k}_1, \mathbf{k}_2) + G(\mathbf{k}_2, \mathbf{k}_3) + G(\mathbf{k}_1, \mathbf{k}_4) + G(\mathbf{k}_3, \mathbf{k}_4) - \\ & - G(\mathbf{k}_1, \mathbf{k}_2 + \mathbf{k}_4) - G(\mathbf{k}_3, \mathbf{k}_2 + \mathbf{k}_4) - G(\mathbf{k}_2, \mathbf{k}_1 + \mathbf{k}_3) - \\ & - G(\mathbf{k}_4, \mathbf{k}_1 + \mathbf{k}_3) + G(\mathbf{k}_1 + \mathbf{k}_3, \mathbf{k}_2 + \mathbf{k}_4)] + \\ & + \delta^{ad}\delta^{bc} [G(\mathbf{k}_1, \mathbf{k}_3) + G(\mathbf{k}_3, \mathbf{k}_4) + G(\mathbf{k}_1, \mathbf{k}_2) + G(\mathbf{k}_2, \mathbf{k}_4) - \\ & - G(\mathbf{k}_1, \mathbf{k}_2 + \mathbf{k}_3) - G(\mathbf{k}_4, \mathbf{k}_2 + \mathbf{k}_3) - G(\mathbf{k}_3, \mathbf{k}_1 + \mathbf{k}_4) - \\ & - G(\mathbf{k}_2, \mathbf{k}_1 + \mathbf{k}_4) + G(\mathbf{k}_1 + \mathbf{k}_4, \mathbf{k}_2 + \mathbf{k}_3)] \Big\}. \quad (2.19) \end{aligned}$$

The convolution $D_2 \otimes G$ is given by the expression [9]

$$(D_2 \otimes G)(\mathbf{a}, \mathbf{b}) = 3g^2 \int \frac{d^2k}{(2\pi)^3} \left\{ \left[\frac{\mathbf{a}^2}{(\mathbf{k} - \mathbf{a})^2 k^2} + \frac{\mathbf{b}^2}{(\mathbf{k} + \mathbf{b})^2 k^2} - \frac{(\mathbf{a} + \mathbf{b})^2}{(\mathbf{k} - \mathbf{a})^2 (\mathbf{k} + \mathbf{b})^2} \right] D_2(\mathbf{k}^2) - \right. \\ \left. - \frac{1}{(\mathbf{k} - \mathbf{a})^2} \left[\frac{\mathbf{a}^2}{(\mathbf{k} - \mathbf{a})^2 + k^2} - \frac{(\mathbf{a} + \mathbf{b})^2}{(\mathbf{k} - \mathbf{a})^2 + (\mathbf{k} + \mathbf{b})^2} \right] D_2(\mathbf{a}^2) - \right. \\ \left. - \frac{1}{(\mathbf{k} + \mathbf{b})^2} \left[\frac{\mathbf{b}^2}{(\mathbf{k} + \mathbf{b})^2 + k^2} - \frac{(\mathbf{a} + \mathbf{b})^2}{(\mathbf{k} - \mathbf{a})^2 + (\mathbf{k} + \mathbf{b})^2} \right] D_2(\mathbf{b}^2) \right\}. \quad (2.20)$$

For the twist analysis in DLA it is useful to perform a Mellin-transformation in the following way (cf. eqn. (2.3)):

$$(D_2 \otimes G)(\omega, \mathbf{a}, \mathbf{b}) = \int \frac{d\nu}{2\pi i} D_2(\omega, \nu) \tilde{G}(\nu, \mathbf{a}, \mathbf{b}) \quad (2.21)$$

with [9]

$$\tilde{G}(\nu, \mathbf{a}, \mathbf{b}) = \frac{3g^2}{(2\pi)^2} \Theta(|\mathbf{a}| - |\mathbf{b}|) \left\{ \left[\ln \left(\frac{|\mathbf{a}|}{|\mathbf{b}|} \right) - \frac{1}{\nu} \right] (b^2)^{-\nu} + \right. \\ \left. + \sum_{n=1}^{\infty} \left(-\frac{|\mathbf{b}|}{|\mathbf{a}|} \right)^n \cos(n\theta) \left[\left(\frac{1}{n+\nu} - \frac{1}{n} \right) (a^2)^{-\nu} + \right. \right. \\ \left. \left. + \left(\frac{1}{n-\nu} - \frac{1}{n} \right) (b^2)^{-\nu} \right] \right\} + (|\mathbf{a}| \leftrightarrow |\mathbf{b}|), \quad (2.22)$$

where θ represents the angle between \mathbf{a} and \mathbf{b} . The leading-twist part in the DLA can be obtained by evaluating the residue at $\nu = -1$:

$$\tilde{G}(\nu, \mathbf{a}, \mathbf{b})^{\tau=2} = -\frac{3g^2}{(2\pi)^2} \mathbf{a} \cdot \mathbf{b} \frac{(\max(a^2, b^2))^{-\nu-1}}{\nu + 1}, \quad (2.23)$$

whereas the twist-four contribution is related to the pole at $\nu = -2$:

$$\tilde{G}(\nu, \mathbf{a}, \mathbf{b})^{\tau=4} = \frac{3g^2}{(2\pi)^2} [2(\mathbf{a} \cdot \mathbf{b})^2 - a^2 b^2] \frac{(\max(a^2, b^2))^{-\nu-2}}{\nu + 2}. \quad (2.24)$$

Inserting the twist-two result (2.23) in (2.19), we find that the sum of the various terms cancel. Returning to (2.18), this cancellation means that we are losing one $\ln Q^2$, i.e. we have a non-leading correction to the DLA which is beyond our control and will therefore be disregarded. For the twist-four result, on the other hand, we find a nonzero coefficient of the pole near $\nu = -2$. In (2.18) the twist-four part of the first term on the r.h.s. reads (we use DLA accuracy, and we

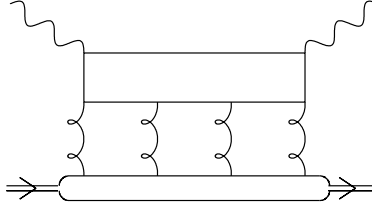


FIG. 2: The four-gluon amplitude at leading order. The fermion-loop symbolizes the sum over all Feynman-diagrams with all possible couplings of the four t -channel gluons.

assume, for simplicity, that all k_i^2 are of the same order, k^2):

$$\begin{aligned}
\frac{1}{\omega} D_2^t \otimes V(\omega; \mathbf{k}_1, \mathbf{k}_2, \mathbf{k}_3, \mathbf{k}_4)^{\tau=4} &= a_2^t \sum_f e_f^2 \frac{\sqrt{8}}{2\pi} 2\sqrt{2} \alpha_s^3 \frac{Q^2}{Q_0^2} \int \frac{d\tilde{\nu}}{2\pi i} \left(\frac{1}{k^2} \right)^{\tilde{\nu}} \frac{1}{\omega \tilde{\nu}} \frac{1}{(\omega \tilde{\nu} - \gamma_2)} \times \\
&\times \{ (-\delta^{ab} \delta^{cd} + \delta^{ac} \delta^{bd} + \delta^{ad} \delta^{bc}) \mathbf{k}_1 \cdot \mathbf{k}_2 \mathbf{k}_3 \cdot \mathbf{k}_4 + \\
&\quad + (\delta^{ab} \delta^{cd} - \delta^{ac} \delta^{bd} + \delta^{ad} \delta^{bc}) \mathbf{k}_1 \cdot \mathbf{k}_3 \mathbf{k}_2 \cdot \mathbf{k}_4 + \\
&\quad + (\delta^{ab} \delta^{cd} + \delta^{ac} \delta^{bd} - \delta^{ad} \delta^{bc}) \mathbf{k}_1 \cdot \mathbf{k}_4 \mathbf{k}_2 \cdot \mathbf{k}_3 \}.
\end{aligned} \tag{2.25}$$

Here $\tilde{\nu} \equiv \nu + 2$, and all momenta are normalized by Q . The factors in the first line of eqn. (2.25) arise from the two-gluon amplitude and the quark-loop in DLA, while the lower three lines correspond to the transition $2 \rightarrow 4$ gluons. A similar result holds for the longitudinal structure function (with a_2^t replaced by b_2^l , and an extra factor $1/\tilde{\nu}$ in the first line).

Making systematic use of the double logarithmic approximation, it is possible to find an explicit solution of eqn. (2.18). To this end we solve the integral equation by iteration: D_4^l then represents a sum of diagrams which have the following structure (fig. 1b). At the top we start with the quark-loop $D_{2,0}$ coupled to a BFKL ladder. At the lower end of this ladder we have the $2 \rightarrow 4$ transition vertex V , then further below the four-gluon state with the sum over all pairwise interactions. It is, now, convenient to use the method of Faddeev [19]. We reorganize the sum over all pairwise gluon interactions and introduce auxiliary potentials $T_{(ij)(kl)}$ which describe pairs of two-gluon ladders between the gluon lines (ij) and (kl) . The original sum over all pairwise interactions between the four gluon lines then translates into the iteration of these auxiliary potentials, allowing for all possible recombinations (“switches”) $(ij)(kl) \rightarrow (ik)(jl)$ etc. For each gluon ladder there are six irreducible color states ($8 \otimes 8 = 1 \oplus 8_A \oplus 8_S \oplus 10 \oplus \bar{10} \oplus 27$). However, if we add the first rung right below the vertex in eqn. (2.25), e.g. between the gluons 1 and 2, and extract the leading power of $\ln(k^2/Q^2)$ the three terms in (2.25) become proportional to $\mathbf{k}_1 \cdot \mathbf{k}_2 \mathbf{k}_3 \cdot \mathbf{k}_4$ and the anti-symmetric color states cancel, so that only the symmetric ones (1, 8_S , 27) survive. This remains true if one adds further rungs. As a result, our four-gluon system has only nine components: three color components for each coupling scheme (12)(34), (13)(24) and (14)(23). Concentrating, now, on the twist-four point $\nu = -2$ and collecting the maximum number of logarithms, we find the following pattern. For each two-ladder state described by the auxiliary potential $T_{(ij)(kl)}$ we have a propagator γ_i :

$$\gamma_i = \left(1 - \frac{4\sigma_i}{\omega \tilde{\nu}} \right)^{-\frac{1}{2}} - 1, \tag{2.26}$$

where $\pi\sigma_i/\alpha_s = \{3, 3/2, -1\}$ for the color states $i = \{1, 8_S, 27\}$. At each switch from the two-ladder state $(ij)(kl)$ to the configuration $(ik)(jl)$, we collect a factor $1/2$ from the angular integration, and insert a color recoupling matrix S . In our nine-component matrix notation, the Green's function Σ for the four-gluon system then becomes:

$$\Sigma = \sum_{n=0}^{\infty} \left(G \frac{1}{2} S \right)^n G = \left(G^{-1} - \frac{1}{2} S \right)^{-1}, \quad G = \begin{pmatrix} \gamma & 0 & 0 \\ 0 & \gamma & 0 \\ 0 & 0 & \gamma \end{pmatrix}, \quad S = \begin{pmatrix} 0 & \Lambda & \Lambda \\ \Lambda & 0 & \Lambda \\ \Lambda & \Lambda & 0 \end{pmatrix}, \quad (2.27)$$

where the sub-matrices γ and Λ have the following components:

$$\gamma = \begin{pmatrix} \left(1 - \frac{4\sigma_1}{\omega\tilde{\nu}}\right)^{-\frac{1}{2}} - 1 & 0 & 0 \\ 0 & \left(1 - \frac{4\sigma_{8_S}}{\omega\tilde{\nu}}\right)^{-\frac{1}{2}} - 1 & 0 \\ 0 & 0 & \left(1 - \frac{4\sigma_{27}}{\omega\tilde{\nu}}\right)^{-\frac{1}{2}} - 1 \end{pmatrix} \quad \Lambda = \begin{pmatrix} \frac{1}{8} & \frac{1}{2\sqrt{2}} & \frac{3\sqrt{3}}{8} \\ \frac{1}{2\sqrt{2}} & -\frac{3}{10} & \frac{3}{10}\sqrt{\frac{3}{2}} \\ \frac{3\sqrt{3}}{8} & \frac{3}{10}\sqrt{\frac{3}{2}} & \frac{7}{40} \end{pmatrix}. \quad (2.28)$$

As a result of the leading- $\ln Q^2$ approximation, at the lower end of the Green's function Σ the two ladder system $T_{(ij)(kl)}$ ends up with the momentum configuration $\mathbf{k}_i = -\mathbf{k}_j \equiv \mathbf{l}$ and $\mathbf{k}_k = -\mathbf{k}_l \equiv \mathbf{l}'$, and for simplicity we set $\mathbf{l}^2 = \mathbf{l}'^2 = Q_0^2/Q^2$.

For the coupling of this Green's function to the transition vertex we introduce the nine component vector \mathbf{V} : $\mathbf{V}^T = (\mathbf{v}^T, \mathbf{v}^T, \mathbf{v}^T)$ with

$$\mathbf{v}^T = (2, 4\sqrt{2}, 6\sqrt{3}). \quad (2.29)$$

This vector is obtained from (2.25) by applying the color projectors listed in the appendix. As a result, our function D_4^I , written as a (transposed) nine component vector, takes the form:

$$\begin{aligned} D_4^{I,t}(\omega, Q_0^2/Q^2) &= \frac{1}{\omega} (D_2^t \otimes \mathbf{V}^T)(\omega, Q^2)^{\tau=4} + \\ &+ a_2^t \sum_f e_f^2 \frac{\sqrt{8}}{2\pi} 2\sqrt{2} \alpha_s^3 \left(\frac{Q_0^2}{Q^2} \right)^2 \int \frac{d\tilde{\nu}}{2\pi i} \left(\frac{Q^2}{Q_0^2} \right)^{\tilde{\nu}} \frac{1}{\omega\tilde{\nu}} \frac{1}{(\omega\tilde{\nu} - \gamma_2)} \cdot \mathbf{V}^T \Sigma(\omega\tilde{\nu}). \end{aligned} \quad (2.30)$$

Finally we have to couple the four-gluon system to the proton. In modelling this coupling we take, as a guideline, the structure of D_4 : to be definite, we assume that the coupling to the proton has the same symmetry properties as D_4 in (2.16), the coupling of the four-gluon state to a perturbative target, e.g. to a virtual photon or to a heavy onium state. The decomposition in (2.16) reflects the different contributions: apart from totally symmetric (under the combined interchange of color and momenta) terms which are contained in D_4^I and D_4^R , we have a term with mixed symmetry properties which occurs only in D_4^R . For the symmetric piece we make the simplest ansatz, which contains only the color singlet representation. For the term with the mixed symmetry we simply follow the perturbative ansatz. This leads to:

$$\varphi_4^{abcd} = \varphi_{4S}^{abcd} + \varphi_{4A}^{abcd} \quad (2.31)$$

with

$$\varphi_{4S}^{abcd} = \frac{1}{3 \cdot 8} \frac{1}{k_1^2 k_2^2 k_3^2 k_4^2} \left(\delta^{ab} \delta^{cd} f_S(1, 2; 3, 4; \omega) + \delta^{ac} \delta^{bd} f_S(1, 3; 2, 4; \omega) + \delta^{ad} \delta^{bc} f_S(1, 4; 2, 3; \omega) \right) \quad (2.32)$$

and

$$\varphi_{4A}^{abcd} = -\frac{1}{3 \cdot 8} \frac{1}{k_1^2 k_2^2 k_3^2 k_4^2} \left(f^{abm} f^{mcd} f_A(1, 2; 3, 4; \omega) + \right. \\ \left. + f^{acm} f^{mbd} f_A(1, 3; 2, 4; \omega) + f^{adm} f^{mbc} f_A(1, 4; 2, 3; \omega) \right) \quad (2.33)$$

with positive-valued functions f_S and f_A . The signs follow from the AGK rules and will be discussed below in more detail. The pre-factors $1/8$ and $1/3$ are convenient for color and for statistics, resp. We immediately see that the φ_{4A} -term does not couple to D_4^I but only to D_4^R , and we will come back to this term when we discuss D_4^R . In order to discuss the momentum structure of the ansatz φ_{4S} , let us recall that in the usual DIS leading-twist ladder the lowest cell has only a longitudinal integration, and the integration over the virtuality of the lowest parton is absorbed into the initial condition $\varphi_2(Q_0^2, x)$. In evaluating our four-gluon system in the DLA we treat each gluon ladder of our auxiliary potential $T_{(ij)(kl)}$ in the same way as the leading-twist ladder. Let the lowest potential be $T_{(12)(34)}$. At its lower end we have the momentum factor $(\mathbf{k}_1 \mathbf{k}_2)(\mathbf{k}_3 \mathbf{k}_4)$. In the function $f_S(i, j; k, l; \omega)$ of our ansatz (2.31) the main contribution comes from the region where

$$\mathbf{k}_i = \mathbf{l} + \mathbf{r}, \quad \mathbf{k}_j = -\mathbf{l} + \mathbf{r}, \quad \mathbf{k}_k = \mathbf{m} - \mathbf{r}, \quad \mathbf{k}_l = -\mathbf{m} - \mathbf{r}, \\ r^2 \ll l^2, m^2. \quad (2.34)$$

Combining these functions with the momentum factors from the auxiliary potential $T_{(12)(34)}$ we are lead to the following definition of our initial condition:

$$Q_0^2 \varphi_{4S}(Q_0^2; \omega) = \int^{Q_0^2} dr^2 \int_{r^2}^{Q_0^2} \frac{dl^2}{l^4} \int_{r^2}^{Q_0^2} \frac{dm^2}{m^4} l^2 m^2 f_S(k_i, k_j; k_k, k_l; \omega). \quad (2.35)$$

Inserting into (2.32) the momentum assignment (2.34), and using the definition (2.35) we get a factor

$$\frac{1}{3 \cdot 8} \left(\delta^{ab} \delta^{cd} + \frac{1}{2} \delta^{ac} \delta^{bd} + \frac{1}{2} \delta^{ad} \delta^{bc} \right) Q_0^2 \cdot \varphi_{4S}(Q_0 r; \omega), \quad (2.36)$$

where the factors $1/2$ in front of the second and the third term are due to the angular integrations over \mathbf{l} and \mathbf{m} (a similar definition holds for the functions φ_{4A} and f_A). As to the longitudinal integrals, since we work in ω -space we allow the function φ_{4S} to depend on ω : if we assume a single ladder to rise as $(1/x)^\lambda$, φ_{4S} should have a pole at $\omega = 2\lambda$, i.e. the initial distribution rises twice as strong as the leading-twist gluon structure function at the same scale.

Finally we couple this ansatz to D_4^I in (2.30). Projecting onto the color eigenstates and introducing the nine-component vector

$$\Phi_{4S}(Q_0^2, \omega) = \begin{pmatrix} \mathbf{w} \\ \mathbf{w} \\ \mathbf{w} \end{pmatrix} \cdot \varphi_{4S}(Q_0^2; \omega), \quad \mathbf{w} = \frac{1}{3 \cdot 8} \begin{pmatrix} 9 \\ 2\sqrt{2} \\ 3\sqrt{3} \end{pmatrix} \quad (2.37)$$

we arrive at the following expression for our twist-four contribution to the structure function in the

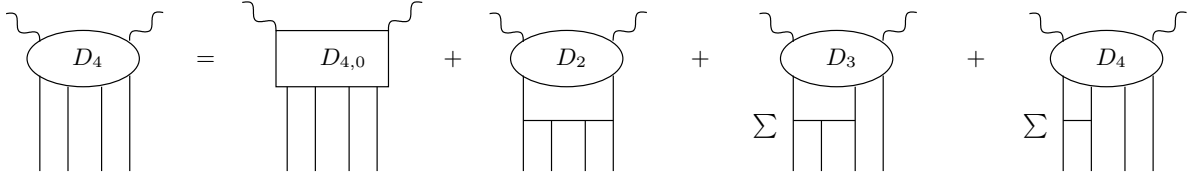


FIG. 3: The integral equation for D_4 . The sums denote couplings to the gluon lines in all possible ways.

(ω, ν) -representation:

$$\begin{aligned}
\Delta F_t^I &= -\frac{1}{128\pi^2} \frac{Q^2}{Q_0^2} D_4^{I;abcd}(\omega, \nu) \varphi_4^{abcd}(\omega) = \\
&= -\frac{a_2^t \alpha_s^3}{16 \pi^3} \sum_f e_f^2 \frac{Q_0^2}{Q^2} \int \frac{d\tilde{\nu}}{2\pi i} \left(\frac{Q^2}{Q_0^2} \right)^{\tilde{\nu}} \frac{1}{\omega \tilde{\nu}} \frac{1}{(\omega \tilde{\nu} - \gamma_2)} \varphi_{4S}(\omega) \\
&\quad - \frac{a_2^t \alpha_s^3}{32 \pi^3} \sum_f e_f^2 \frac{Q_0^2}{Q^2} \int \frac{d\tilde{\nu}}{2\pi i} \left(\frac{Q^2}{Q_0^2} \right)^{\tilde{\nu}} \frac{1}{\omega \tilde{\nu}} \frac{1}{(\omega \tilde{\nu} - \gamma_2)} \cdot \mathbf{V}^T \Sigma(\omega \tilde{\nu}) \Phi_{4S}(\omega),
\end{aligned} \tag{2.38}$$

and an analogous expression in the longitudinal case. After performing the inversion within $\Sigma = (G^{-1} - \frac{1}{2}S)^{-1}$ we get explicit expressions for the components of vector $\Sigma \mathbf{V}$. They are listed in the appendix.

As one of the most striking features of (2.38) we note that Σ has a leading singularity in the $\tilde{\nu}$ -plane at [16, 20]

$$\tilde{\nu} = 4(1 + \delta) \frac{N_c \alpha_s}{\pi \omega}, \tag{2.39}$$

where $\delta = 0.009549$. Using the usual saddle point approximation, this pole leads to the following asymptotic small x behavior:

$$D_4^I \sim \left(\frac{Q_0^2}{Q^2} \right)^2 \exp \left(2 \left(1 + \frac{\delta}{2} \right) \sqrt{\frac{4N_c}{\pi} \alpha_s \ln(1/x) \ln(Q^2/Q_0^2)} \right). \tag{2.40}$$

This rise at small x is approximately twice as strong as that of the leading-twist gluon structure function, and at sufficiently small x the four-gluon higher-twist term will become as strong as the leading-twist term, despite its suppression coming from the extra power in α_s and the $1/Q^2$ factor. This strong rise at small x is the reason why the four-gluon operator, (2.1), is expected to be so important in the small x , low Q^2 -region.

Besides the leading pole (2.39), there are more singularities in the $\tilde{\nu}$ -plane, which have been discussed in some detail in ref. [21]. There are three cuts in the $\tilde{\nu}$ -plane. The first one stems from the singlet-part of matrix γ (eqn. (2.28)). It starts at $\tilde{\nu} = 0$ and goes up to the point $\tilde{\nu} = 4 \frac{N_c \alpha_s}{\pi \omega}$ which is very close to the leading pole (2.39). It overlaps with the symmetric color octet cut, which is located in the interval $[0, \frac{6\alpha_s}{\pi \omega}]$. Finally, the cut of the color 27plet goes from $-\frac{4\alpha_s}{\pi \omega}$ to 0.

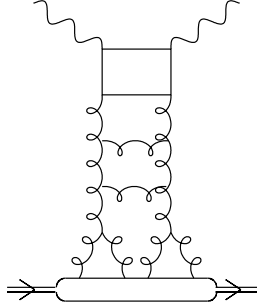


FIG. 4: The reggeizing part of the four-gluon amplitude has the same evolution as the two-gluon amplitude but is suppressed by one factor α_s .

Finally, we return to (2.16) and we discuss the *reducible* part D_4^R . From [9, 16] we have:

$$\begin{aligned}
 D_4^R(\mathbf{k}_1, \mathbf{k}_2, \mathbf{k}_3, \mathbf{k}_4) = & \quad (2.41) \\
 = \frac{g^2}{2\sqrt{2}} \left\{ & d^{abcd} [D_2(\mathbf{k}_1, \mathbf{k}_2 + \mathbf{k}_3 + \mathbf{k}_4) + D_2(\mathbf{k}_4, \mathbf{k}_1 + \mathbf{k}_2 + \mathbf{k}_3) - D_2(\mathbf{k}_1 + \mathbf{k}_4, \mathbf{k}_2 + \mathbf{k}_3)] + \right. \\
 & + d^{abdc} [D_2(\mathbf{k}_2, \mathbf{k}_1 + \mathbf{k}_3 + \mathbf{k}_4) + D_2(\mathbf{k}_3, \mathbf{k}_1 + \mathbf{k}_2 + \mathbf{k}_4) - D_2(\mathbf{k}_1 + \mathbf{k}_2, \mathbf{k}_3 + \mathbf{k}_4) - \\
 & \left. - D_2(\mathbf{k}_1 + \mathbf{k}_3, \mathbf{k}_2 + \mathbf{k}_4)] \right\},
 \end{aligned}$$

where the color tensor d^{abcd} is given in the appendix. It contains both symmetric pieces and pieces with mixed symmetry: one easily recognizes the structures (2.32) and (2.33). Convoluting D_4^R with our ansatz (2.31) we find that φ_{4S} couples only to the symmetric and φ_{4A} only to the mixed-symmetric part of D_4^R . With the help of the same arguments as before, cf. (2.35), we arrive at

$$\begin{aligned}
 \Delta F_t^R = & -\frac{1}{128\omega\pi^2} \left(\frac{Q^2}{Q_0^2} \right) D_4^{R;abcd} \varphi_4^{abcd}(\omega)^{\tau=4} = \\
 = & \frac{a_2^t \alpha_s^2}{64 \pi^2} \sum_f e_f^2 \frac{1}{\omega} \left(\frac{Q_0^2}{Q^2} \right) \exp\left(\frac{\gamma_2}{\omega} \ln(Q^2/Q_0^2) \right) \frac{1}{3} [14\varphi_{4S}(\omega) - 9\varphi_{4A}(\omega)]. \quad (2.42)
 \end{aligned}$$

Here φ_{4A} is defined in analogy with φ_{4S} in (2.35). It is important to note that the negative sign in front of φ_{4A} is dictated by the AGK rules (see below). Note that, to lowest order in α_s , it is this contribution D_4^R that contains the diagrams with four elementary gluon lines between the quark-loop and the proton (fig. 2).

Having written down our DLA expressions for the four-gluon twist-four contributions, we briefly return to the operator product expansion. As before, the ladder diagrams denote the $\ln Q^2$ evolution in the DLA, but instead of writing the four-gluon amplitude as an evolution equation in $\ln Q^2$ we have used the closed expression in the (ω, ν) -representation. Twist-four corresponds to the point $\nu = -2$. D_4^I then has the following interpretation: the upper two-gluon ladder (evaluated near $\nu = -2$) describes the evolution of operator (2.2), the $2 \rightarrow 4$ vertex the mixing between (2.1) and (2.2), and the Green's function Σ the evolution of the four-gluon operators (2.1). Obviously, the three auxiliary potentials $T_{(12)(34)}$, $T_{(13)(24)}$, $T_{(14)(23)}$ belong to the three operators in the first, second, and third line of (2.1), and what we have called “switching from $(ij)(kl)$ to $(ik)(jl)$ ” has

to be interpreted as the mixing between these three different four-gluon operators. If we were to go beyond DLA, there would also be a transition from the four-gluon state back to two gluons (this vertex could again be derived from (2.19) and (2.22), by expanding about $\nu = 1$), and eventually these transitions would be iterated and exponentiated in the t -channel. A remarkable feature of the small x approximation (upon which the DLA is based) is the fact that the four-gluon operator has no direct coupling to the quark-loop. Our ansatz (2.31) for the coupling to the proton, i.e. for the initial condition, which we so far have motivated by inspecting the structure of D_4 , also arises from an analysis in the spirit of [7]: the matrix element of the product of four-gluon fields has to be decomposed into terms with different symmetry properties.

The interpretation of the contribution D_4^R , on the other hand, is more subtle. As stated before, this term has its origin in the reggeization of the gluon: from the point of view of DIS the appearance of reggeization is a “novel” phenomenon since at the leading-twist level it has played only an indirect rôle (e.g. as part of the NLO anomalous dimension of the gluon). From the point of view of Q^2 evolution, D_4^R belongs to the two-gluon operator (2.2). Including D_4^R , therefore, at first sight seems like adding a non-leading correction to (2.15), and within the DLA we better should restrict ourselves to the leading term (2.15). On the other hand, the analysis in [9] clearly shows that D_4^I and D_4^R have the same origin (diagrams with four gluons in the t -channel) and come with the same powers of logarithms. We, therefore, believe that for the twist-four calculations – which necessarily have to include t -channel states with four gluons – we have to keep D_4^R as a separate contribution, in addition to (2.15).

A better understanding of why we have to keep this contribution can be obtained by looking at the evolution of the gluonic operator in (2.2). The mixing between (2.1) and (2.2) is of order α_s^2 in the anomalous dimension matrix, i.e. in total the correction to the evolution of (2.2) due to the transition from (2.2) to (2.1) and back to (2.2) is a NNLO effect of order α_s^3 . To be consistent, we, therefore, have to include NNLO corrections also in the anomalous dimension $\gamma^{\tau=4}$ in (2.8) and in the coefficient function. They are not available yet. On the other hand, what we are seeing in D_4^R can be viewed as a particular piece of these corrections, connected with the reggeization of the gluon. Moreover, there are reasons to expect that they are the most important ones. Since we are studying t -channel states with four gluons, D_4^R provides contributions from the “decay of a reggeizing gluon into two or three gluons” which then become partons inside the proton. In other words, we are encountering the two- and three-particle states in the gluon trajectory function, appearing at the lower end of the two-gluon ladder. Clearly, these higher-order particle states in the trajectory function can appear not only at the lower end of the two-gluon ladder (as taken into account by D_4^R) but also somewhere between the proton and the photon. Such a contribution would then be part of the NNLO corrections to the gluon rung, i.e. to the anomalous dimension $\gamma^{\tau=4}$ in (2.8) mentioned above. In this sense, D_4^R counts those NNLO corrections to the two-gluon kernel which are connected with four-gluon states in the t -channel, and these corrections are taken into account only at the lower end of the ladder. When running α_s and the strong ordering of the transverse momenta is taken into account, we expect these corrections to be largest when they appear at the lower end of the ladder. For these reasons our incomplete treatment of the NNLO corrections in the evolution of the two-gluon operator (2.2) may not be such a bad approximation.

2.3 Contributions with Three t -channel Gluons

Since there are no three-gluon operators that might contribute to our twist-four analysis of the unpolarized structure functions, t -channel states with three gluons can come in only through the mechanism which we have discussed at the end of the previous section. In the evolution equations of the two-gluon operator (2.2) we should include the NLO corrections to the anomalous dimension $\gamma^{\tau=4}$ in (2.8) as well as to the coefficient function. Whereas the former ones are, at least in principle, now available (so far, they have not been computed from [17]; as pointed out in [22], it is not clear how the behavior near $\nu = -1$ can directly be extracted from the results of [17]), NLO corrections to the coefficient function are not known. In our analysis, therefore, we follow the same logic as for the four-gluon case. From [9] we know scattering amplitudes with three gluons in the t -channel (in [9] they are called D_3). Because of the reggeization of the gluon they can also be written as a sum of D_2 functions (cf. (2.41)):

$$D_3(\mathbf{k}_1, \mathbf{k}_2, \mathbf{k}_3) = \frac{g}{4\sqrt{2}} f^{abc} (D_2(\mathbf{k}_1 + \mathbf{k}_2, \mathbf{k}_3) + D_2(\mathbf{k}_1, \mathbf{k}_2 + \mathbf{k}_3) - D_2(\mathbf{k}_1 + \mathbf{k}_3, \mathbf{k}_2)). \quad (2.43)$$

The convolution with the initial distribution of the proton requires a new function, $\varphi_3(\omega)$. One ends up with functions $\Delta F_{(t,\ell)}^3$ that have the same dependence on variables as (2.42) (with a different constant factor in front of the r.h.s.; it will be absorbed into the unknown initial distribution φ_3).

2.4 Running α_s

Since in DLA the leading-twist two-gluon amplitude must coincide with the DGLAP solution, it is clear how one can consider the fact that α_s is running in this case. One has to exchange the value of fixed α_s by $\bar{\alpha}_s \equiv 4\pi/\beta_0$ ($\gamma_2 \rightarrow 12/\beta_0$) and the expression Q^2/Q_0^2 by t/t_0 , where $t = \ln(Q^2/\Lambda^2)$ and $t_0 = \ln(Q_0^2/\Lambda^2)$. This procedure should be applicable for the bare four-gluon amplitude (i.e. the amplitude without two-gluon amplitude and vertex at the top of fig. 1b), as well, since the addition of one rung is always performed by convolution with the common BFKL kernel. This means that every time α_s comes with a factor $\ln(t/t_0)$ it has to be replaced by $\bar{\alpha}_s$.

There are three powers of α_s in eqn. (2.38): One stems from the quark-loop, which (in the longitudinal case at leading order) is proportional to a logarithm. The remaining two powers stem from the coupling of the four-gluon to the two-gluon amplitude via the Vertex V (fig. 1b). Here we get only one logarithm. We write this coupling symbolically as

$$D_4^{I,\ell} = \int_{\tau_0}^{\tau} d\tau' \exp[\gamma_2(\tau - \tau')] f \alpha_s^2 \int \frac{d\nu}{2\pi i} \exp[\nu(\tau' - \tau_0)] G(\nu), \quad (2.44)$$

where $\tau = \ln t$ etc., $G(\nu)$ is understood as the *four-gluon amplitude Greens-function* and f shall contain all remaining factors. In eqn. (2.44) one factor α_s needs to be replaced by $\alpha_s(t')$ and the other one by $\bar{\alpha}_s$. If, on the other hand, we go back to fixed α_s , we have to replace τ and τ' in eqn. (2.44) by t and t' , resp. Performing the t' -integration and comparing with eqn. (2.38), we can identify the quantities G and f . By this way we arrive at the following conclusions: For running α_s the factor $(Q^2/Q_0^2)^\nu$ in eqn. (2.38) has to be replaced by $(t/t_0)^\nu$, one power α_s has to be evaluated as $\alpha_s(Q^2)$, while (in the longitudinal case) the remaining two powers are replaced by $\bar{\alpha}_s$. In the denominators we have to replace the factor $(\omega\nu - \gamma_2)$ by $(\omega\nu - \omega - \gamma_2)$.

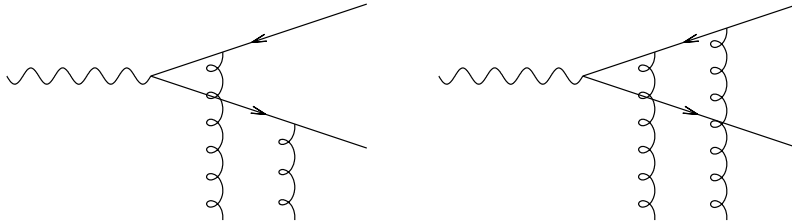


FIG. 5: Two of the four diagrams which enter into diffractive $q\bar{q}$ -production at leading order.

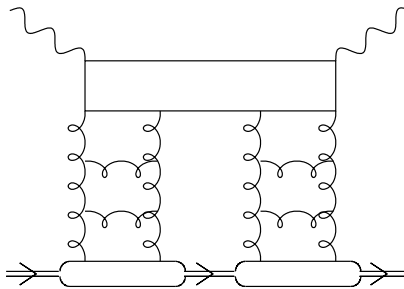


FIG. 6: The twist-four part of diffractive $q\bar{q}$ -production is described by exchange of gluon ladders.

Repeating in (2.30) the standard saddle point analysis (cf. eqn. (2.39)), we arrive at a small x behavior of the form

$$D_4^I \sim \left(\frac{Q_0^2}{Q^2}\right)^2 \exp \left[2 \left(1 + \frac{\delta}{2}\right) \sqrt{\frac{48}{\beta_0} \ln \frac{1}{x} \ln \frac{t}{t_0}} \right]. \quad (2.45)$$

Apart from the small δ -correction, this small x behavior is just the square of the well-known leading-twist double scaling formula [23, 24]. Therefore, in the kinematical regime in which D_4^I gives the main contribution to twist-four, higher-twist is expected to increase much faster with decreasing x than leading-twist and to decrease slower than $1/Q^2$.

We end this section with a brief summary. All in all we have collected four different contributions (both for the transverse and the longitudinal structure function). In our notation

$$\Delta F = \Delta F^{(2)} + \Delta F^{(3)} + \Delta F^R + \Delta F^I, \quad (2.46)$$

where we have suppressed labels t and ℓ . As far as the Q^2 -evolution is concerned, the first three terms belong to the twist-four two-gluon operator (2.2) whereas the last one belongs to the four-gluon operators (2.1). This last contribution is of particular interest, since at small x it rises stronger than the other ones and, therefore, may potentially become large. However, we have already seen that the four contributions in (2.46) come with alternating signs, which hints at the possibility of strong cancellations.

3 Diffractive Dissociation

Up to now, we have been describing the four contributions to twist-four, which we believe to dominate at small x : D_4^R , D_4^I , D_3 and the twist-four part of the two-gluon amplitude. Next, we

Contribution	Sign	$\ln(Q^2/Q_0^2)$	$\beta \rightarrow 1$
Trans. $\tau = 2$	+	non-pert.	vanishes
Trans. $\tau = 4$	-	no	vanishes
Long. $\tau = 2$	vanishes	vanishes	vanishes
Long. $\tau = 4$	+	yes	constant

TABLE 2: The four contributions to diffractive $q\bar{q}$ -production up to twist $\tau = 4$ enter with different signs into the diffractive cross section. The table shows also which contributions have leading logarithms, and how they behave for $\beta \rightarrow 1$.

have to address the important question of specifying the initial distributions φ . Following the conventional leading-twist analysis, we would determine the initial conditions from a fit to the data. In this first attempt of analysing the influence of twist-four corrections at low Q^2 and small x , we will try to estimate the φ functions with the help of empirical data on final states which are known to belong to twist-four. The best candidates for this are diffractive final states, in particular the production of longitudinal vector particles and the production of jets with large transverse momenta. In this section we, therefore, give a brief overview over the rôle of higher-twist in DIS diffraction. In particular, we will discuss the relation between the higher-twist pieces of diffractive cross sections and the higher-twist contributions to F_t and F_ℓ from the previous section. In our numerical analysis these relationships will be used to estimate the initial distribution $\varphi_{4S,A}$.

3.1 Diffractive $q\bar{q}$ -Production

It is useful to divide the kinematical regime into different regions of the variable $\beta \equiv Q^2/(M^2 + Q^2)$, where M is the invariant mass of the diffractive system. We begin with the small mass region ($\beta \rightarrow 1$), where the $q\bar{q}$ -production process is expected to give the main contribution to diffraction. Those contributions to the cross section, which can be calculated perturbatively, can be described as follows. Seen from the angle of the proton rest frame the virtual photon splits up into a $q\bar{q}$ -pair, which interacts with the proton before the quarks result into the two jets. For diffraction the interaction between the $q\bar{q}$ -pair and the proton must be colorless and, therefore, in the small x regime where gluons are expected to dominate, at least two gluons need to be exchanged (fig. 5). The cross section can, now, be computed by coupling the gluons in fig. 5 to the proton and by squaring the diagrams afterwards. This leads to the following expressions in the case of zero momentum transfer ($t = 0$) [25, 26]:

$$\left. \frac{d\sigma^t}{dM^2 dt dp_t^2} \right|_{t=0} = \sum_f e_f^2 \frac{\alpha_{em} \pi^2 \alpha_s^2}{12} \frac{1}{M^4} \frac{\left(1 - \frac{2p_t^2}{M^2}\right)}{\sqrt{1 - \frac{4p_t^2}{M^2}}} \left[- \int \frac{dl^2}{l^2} \mathcal{F}_G(x_P, l^2) \mathcal{I}^t(Q^2, M^2, p_t^2, l^2) \right]^2 \quad (3.1)$$

and

$$\left. \frac{d\sigma^\ell}{dM^2 dt dp_t^2} \right|_{t=0} = \sum_f e_f^2 \frac{\alpha_{em} \pi^2 \alpha_s^2}{3} \frac{4}{Q^2 M^2} \frac{p_t^2}{M^2} \frac{1}{\sqrt{1 - \frac{4p_t^2}{M^2}}} \left[- \int \frac{dl^2}{l^2} \mathcal{F}_G(x_P, l^2) \mathcal{I}^\ell(Q^2, M^2, p_t^2, l^2) \right]^2. \quad (3.2)$$

Here \mathbf{p}_t is the transverse part (in the Sudakov decomposition) of the quark-momenta, $x_{\mathbb{P}} = x_{\mathbb{B}}/\beta$,

$$\mathcal{I}^t(Q^2, M^2, p_t^2, l^2) = \frac{M^2 - Q^2}{M^2 + Q^2} + \frac{l^2 + \frac{p_t^2}{M^2}(Q^2 - M^2)}{\sqrt{\left[l^2 + \frac{p_t^2}{M^2}(Q^2 - M^2)\right]^2 + 4p_t^4 \frac{Q^2}{M^2}}}, \quad (3.3)$$

$$\mathcal{I}^\ell(Q^2, M^2, p_t^2, l^2) = \frac{Q^2}{M^2 + Q^2} - \frac{p_t^2 Q^2}{M^2 \sqrt{\left[l^2 + \frac{p_t^2}{M^2}(Q^2 - M^2)\right]^2 + 4p_t^4 \frac{Q^2}{M^2}}} \quad (3.4)$$

and \mathcal{F}_G represents the unintegrated gluon distribution of the proton

$$\int^{Q^2} dl^2 \mathcal{F}_G(x_{\mathbb{P}}, l^2) = x_{\mathbb{P}} g(x_{\mathbb{P}}, Q^2). \quad (3.5)$$

In order to establish a connection with the deep inelastic structure functions we have to integrate over M^2 (or β), p_t^2 and t . Performing in eqns. (3.1) and (3.2) the p_t^2 - and M^2 -integrations one arrives at the quark-loop at the top of fig. 6, with the constraint that the two-gluon systems at the r.h.s. and at the l.h.s. are in a color singlet state. We denote this with the help of the superscript $(1, +, +)$: $D_{4,0}^{(1,+,+)}$. In terms of $D_{4,0}^{(1,+,+)}$ the integrated diffractive cross section becomes:

$$\left. \frac{d\sigma^{q\bar{q}}}{dt} \right|_{t=0} = \frac{4\pi^2 \alpha_{\text{em}}}{128\pi^2} \int \frac{dl^2}{l^2} \int \frac{dm^2}{m^2} D_{4,0}^{(1,+,+)}(\mathbf{l}, -\mathbf{l}, \mathbf{m}, -\mathbf{m}) \mathcal{F}_G(x_{\mathbb{P}}, l^2) \mathcal{F}_G(x_{\mathbb{P}}, m^2) \quad (3.6)$$

(we have suppressed the distinction between longitudinal and transverse polarization). As shown in [9], $D_{4,0}^{(1,+,+)}(\mathbf{k}_1, \mathbf{k}_2, \mathbf{k}_3, \mathbf{k}_4)$ can be written as a sum of $D_{2,0}$ expressions with appropriate evaluation of momenta:

$$D_{4,0}^{(1,+,+)}(\mathbf{k}_1, \mathbf{k}_2, \mathbf{k}_3, \mathbf{k}_4) = g^2 \frac{\sqrt{2}}{3} \left\{ \begin{aligned} &D_{2,0}(\mathbf{k}_1, \mathbf{k}_2 + \mathbf{k}_3 + \mathbf{k}_4) + D_{2,0}(\mathbf{k}_2, \mathbf{k}_1 + \mathbf{k}_3 + \mathbf{k}_4) + \\ &+ D_{2,0}(\mathbf{k}_3, \mathbf{k}_1 + \mathbf{k}_2 + \mathbf{k}_4) + D_{2,0}(\mathbf{k}_4, \mathbf{k}_1 + \mathbf{k}_2 + \mathbf{k}_3) - \\ &- D_{2,0}(\mathbf{k}_1 + \mathbf{k}_2, \mathbf{k}_3 + \mathbf{k}_4) - D_{2,0}(\mathbf{k}_1 + \mathbf{k}_3, \mathbf{k}_2 + \mathbf{k}_4) - \\ &- D_{2,0}(\mathbf{k}_1 + \mathbf{k}_4, \mathbf{k}_2 + \mathbf{k}_3) \end{aligned} \right\}. \quad (3.7)$$

Here $\mathbf{k}_1, \dots, \mathbf{k}_4$ are the transverse components of the gluon momenta at the lower end of the quark-loop. In our case the quark-loop is coupled to the proton through the unintegrated gluon structure function \mathcal{F}_G (cf. (3.1) and (3.2)), and we have to substitute $\mathbf{k}_1 = -\mathbf{k}_2 = \mathbf{l}$ and $\mathbf{k}_3 = -\mathbf{k}_4 = \mathbf{l}'$ and integrate over \mathbf{l} and \mathbf{l}' . To define leading-twist and twist-four corrections we simply expand in powers of $1/Q^2$.

Before we describe the formal expansion in inverse powers of Q^2 , let us give a qualitative description [27]. We begin with the p_t^2 -integral of the transverse cross section (3.1) and keep M^2 fixed. As long as p_t^2 is not small, the leading contribution of the \mathbf{l} -integral comes from the region of small $l^2 < p_t^2(M^2 + Q^2)/M^2$ where \mathcal{I}^t/l^2 behaves as a constant. The \mathbf{l} -integral, therefore, simply leads to $x_{\mathbb{P}} g(x_{\mathbb{P}}, p_t^2(Q^2 + M^2)/M^2)$, and the transverse cross section falls as $[1/p_t^2 x_{\mathbb{P}} g(x_{\mathbb{P}}, p_t^2(Q^2 + M^2)/M^2)]^2$. Using naive dimensional arguments it follows that this region belongs to higher-twist. Taking the integral over p_t^2 one finds dominance of the low p_t^2 region where perturbation theory

breaks down. The leading-twist of the transverse cross section is obtained by extending the convergent p_t^2 -integral up to infinity. The twist-four term arises as a correction: the correct upper limit to the p_t^2 -integral is $Q^2(1-\beta)/\beta$, i.e. we have to subtract the integral from $Q^2(1-\beta)/\beta$ to infinity. This is the negative twist-four correction to the transverse cross section. The convergence of the p_t^2 -integration implies also that there is no $\ln Q^2$ in the twist-four correction to the transverse cross section. Turning to the longitudinal cross section, one notices in (3.2) the extra p_t^2 factor in front of the square brackets: this changes, compared to the transverse case, the p_t^2 -behavior of the cross section in two ways. When integrating over p_t^2 , the small p_t^2 region no longer dominates, whereas in the large p_t^2 -region we encounter a logarithmic divergence. This explains the $1/Q^2$ -suppression of the cross section and the appearance of a $\ln Q^2$. The β (or M^2) dependence of the two cross sections arises from a closer inspection of the two formulae (3.1) and (3.2): whereas the transverse cross section (both leading- and higher-twist) vanishes near $\beta = 1$, the longitudinal one stays finite. This leads to the conclusion that the longitudinal cross section (which for $\beta \ll 1$ is much smaller than the transverse one) dominates in the large β -region. In other words, the diffractive $q\bar{q}$ cross section near $\beta = 1$ is mainly longitudinal and belongs to twist-four. Results of this discussion are summarized in table 2.

In order to obtain quantitative expressions for the higher-twist cross sections (and to verify our intuitive arguments), we return to the p_t^2 and β -integrated expressions in (3.7) and perform a formal expansion in powers of $1/Q^2$. Using the (ω, ν) -representation for $D_{2,0}$ in (3.7) and expanding about the twist-four point $\nu = -2$ yields for the transverse case

$$\frac{1}{\omega} D_{4,0}^{t(1,+,+)}(\omega, l^2, l'^2)^{\tau=4} = a_2^t \frac{4\pi\sqrt{2}}{3} \frac{1}{\omega} \sum_f e_f^2 \frac{\sqrt{8}}{2\pi} \alpha_s^2 \left\{ 2l^4 + 2l'^4 - (\mathbf{l} + \mathbf{l}')^4 - (\mathbf{l} - \mathbf{l}')^4 \right\}. \quad (3.8)$$

Similarly, in the longitudinal case we get

$$\begin{aligned} \frac{1}{\omega} D_{4,0}^{\ell(1,+,+)}(\omega, l^2, l'^2)^{\tau=4} = & -b_2^\ell \frac{4\pi\sqrt{2}}{3} \frac{1}{\omega} \sum_f e_f^2 \frac{\sqrt{8}}{2\pi} \alpha_s^2 \left\{ 2l^4 \ln l^2 + 2l'^4 \ln l'^2 - \right. \\ & \left. - (\mathbf{l} + \mathbf{l}')^4 \ln(\mathbf{l} + \mathbf{l}')^2 - (\mathbf{l} - \mathbf{l}')^4 \ln(\mathbf{l} - \mathbf{l}')^2 \right\}. \end{aligned} \quad (3.9)$$

Here, l^2 and l'^2 are normalized by Q^2 . Working in DLA, we have for the unintegrated gluon structure function \mathcal{F}_G an expression of the form

$$\mathcal{F}_G(x, l^2) = \frac{1}{Q^2} \frac{\partial}{\partial l^2} \int \frac{d\omega}{2\pi i} \left(\frac{1}{x} \right)^\omega \exp\left(\frac{\gamma_2}{\omega} \ln l^2 / q_0^2 \right) \varphi_2(\omega)^{\tau=2}, \quad (3.10)$$

where $\varphi_2(\omega)$ is the initial distribution of the gluon structure function and $q_0^2 = Q_0^2/Q^2$. Multiplying (3.8) with functions $\mathcal{F}_G(l^2)$ and $\mathcal{F}_G(l'^2)$ and performing the integrations over \mathbf{l} and \mathbf{l}' , we arrive at the following higher-twist correction to the differential diffractive cross section:

$$\Delta \left. \frac{d\sigma^{q\bar{q},t}}{dt} \right|_{t=0} = -\frac{4\pi^2 \alpha_{em}}{Q^4} \frac{a_2^t}{6\pi^2} \frac{\alpha_s^2}{\omega} \sum_f e_f^2 \exp\left(2 \frac{\gamma_2}{\omega} \ln Q^2 / Q_0^2 \right) [\varphi_2(Q_0^2, \omega)]^2. \quad (3.11)$$

For the longitudinal case the \mathbf{l} , \mathbf{l}' integrals are slightly more complicated, since (3.9) contains logarithms. In order to obtain the maximum number of logarithms, we split the integration interval

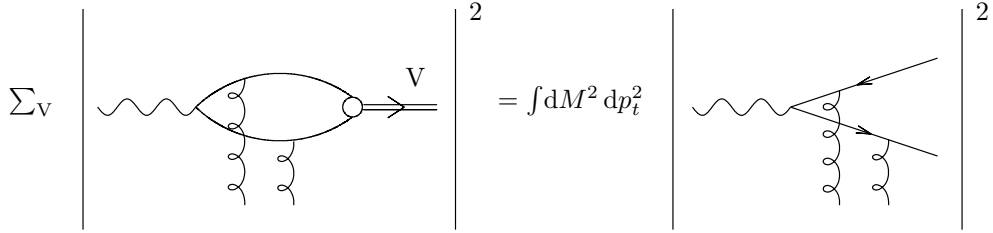


FIG. 7: Duality relates the diffractive vector meson production cross section to the diffractive $q\bar{q}$ -production cross section.

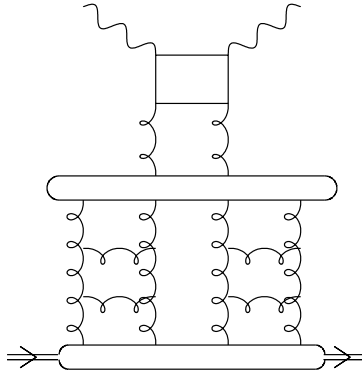


FIG. 8: The (integrated) $q\bar{q}g$ -production amplitude is given by an expression which is symbolized by this figure. Note that the effective $2 \rightarrow 4$ transition vertex is not the same as in fig. 1b for D_4^I .

into subintervals $l^2 < l'^2$ and $l'^2 < l^2$. The result is

$$\Delta \frac{d\sigma^{q\bar{q},\ell}}{dt} \Big|_{t=0} = \frac{4\pi^2 \alpha_{\text{em}}}{Q^4} \frac{b_2^\ell}{6\pi^2} \frac{\alpha_s^2}{2\gamma_2} \sum_f e_f^2 \left\{ 1 - \exp\left(2\frac{\gamma_2}{\omega} \ln Q^2/Q_0^2\right) \right\} [\varphi_2(Q_0^2, \omega)]^2. \quad (3.12)$$

Before we can draw the relation with the inclusive structure functions we still have to integrate over the momentum transfer t . Repeating the discussion in the sequel of eqn. (2.33), we note that in DLA the nonzero momentum transfer enters only into the lowest part of the ladders, the initial distributions φ_2 . Integration in (3.11) or (3.12) over t , therefore, simply means replacing φ_2^2 by $\int d^2\mathbf{q} \varphi_2^2$, i.e. by an effective new initial condition. Moreover, if we allow for diffractive dissociation of the target proton, this initial condition will again be modified into a new initial condition which we denote by $\varphi_4^{\text{diff}}(\omega)$:

$$\Delta \sigma^{q\bar{q},\ell} = \frac{4\pi^2 \alpha_{\text{em}}}{Q^2} \frac{b_2^\ell}{6\pi^2} \frac{\alpha_s^2}{2\gamma_2} \sum_f e_f^2 \frac{Q_0^2}{Q^2} \left\{ 1 - \exp\left(2\frac{\gamma_2}{\omega} \ln Q^2/Q_0^2\right) \right\} \varphi_4^{\text{diff}}(Q_0^2, \omega) \quad (3.13)$$

(and a similar expression for the transverse cross section). Further below we shall discuss how this diffractive cross section contributes to the structure functions $F_{\ell,t}$. In particular, we will derive a relation between $\varphi_4^{\text{diff}}(\omega)$ and $\varphi_{4S,A}(\omega)$ introduced in (2.31).

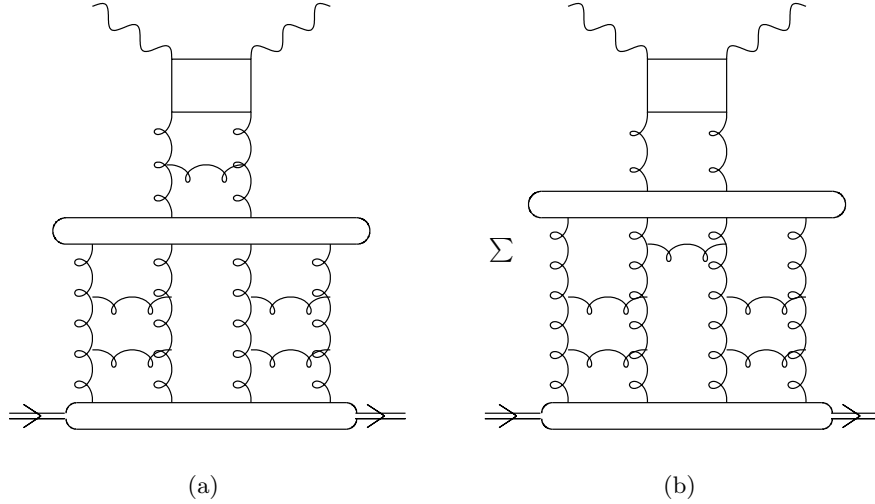


FIG. 9: Same as in fig.8 but now for $q\bar{q}gg$ -production. The sum denotes all possible couplings between systems (12) and (34).

3.2 Diffractive Vector Meson Production

Let us, now, turn to those diffractive processes which have been examined most intensively both theoretically and experimentally, the diffractive production of vector mesons: $\gamma^* + p \rightarrow V + p$, where V can be any vector meson. For the longitudinal photon this process has been shown to be calculable within perturbative QCD [10–13]:

$$\left. \frac{d\sigma_{\gamma^* p \rightarrow V p}^\ell}{dt} \right|_{t=0} = \frac{12\pi^3 \alpha_s^2}{N_c^2 \alpha_{\text{em}}} \frac{M_V}{Q^6} \Gamma_{V \rightarrow e^+ e^-} T(Q^2) \eta_V^2 \left| \left(1 + i \frac{\pi}{2} \frac{d}{d \ln x} \right) xg(x, Q^2) \right|^2. \quad (3.14)$$

Experiments show that the sum over all vector particles gives a significant (about 20 %) contribution to the total diffractive cross section. As can be seen in (3.14), for an individual vector particle, the cross section goes as $1/Q^6$. In ref. [13] it has been shown that the production cross section of a single vector particle can also be obtained if one starts with open $q\bar{q}$ -production and projects onto the corresponding angular momentum and parity quantum numbers. This suggests to apply a simple duality argument and to set, for the mass range $m_\rho < M < M_c$, the sum over vector particle production cross sections (3.14) equal to the M^2 - (and p_t^2 -) integrated cross section of open $q\bar{q}$ -production (3.2) (we illustrate this equality in fig. 7). In this way, the sum over the vector particle cross sections turns into a twist-four contribution: the additional factor $1/Q^2$ in (3.14) is due to the projection onto the vector particle wave function. As a result of this argument, we can use the sum of the measured vector particle cross section to obtain a lower bound of the integrated longitudinal $q\bar{q}$ cross section [28], which has been shown to belong to twist-four.

3.3 Diffractive $q\bar{q}g$ -Production and Multi-Jet Processes

Diffractive $q\bar{q}$ -production is expected to be dominant near $\beta = 1$. If we go to $\beta < 1$, we have to consider also gluon production processes ($q\bar{q}g$ -, $q\bar{q}gg$ -, ... -jets). Cross sections for these processes

Contribution	Sign	$\ln(Q^2/Q_0^2)$	
Trans. $\tau = 2$	+	$\ln(Q^2/Q_0^2)$	non-pert.
Trans. $\tau = 4$	+	$\ln(Q^2/Q_0^2)$	
Long. $\tau = 2$	+	no	non-pert.
Long. $\tau = 4$	-	$(\ln(Q^2/Q_0^2))^2$	

TABLE 3: The four contributions to diffractive $q\bar{q}g$ -production. We list the sign structure and powers of $\ln Q^2$.

have been calculated in different kinematical regions: for very small β (the triple Regge region) in [9, 29], for strong ordering in the transverse momenta in [30, 31]. The latter calculation allows to describe the whole β -interval, but only the first one contains both leading-twist and twist-four. In this section, therefore, we make use only of the results obtained in [29] and discuss the higher-twist contributions to diffractive $q\bar{q}g$ -production. The calculations are done in analogy to the $q\bar{q}$ -production process discussed above: we keep all powers in the transverse momenta, but we restrict ourselves to the leading log in M^2 (or $1/\beta$). An example of the Feynman diagrams is shown in fig. 10a. A complete description can be found in [29]. In general, the s -channel gluon can be emitted anywhere from one of the t -channel gluons.

The analytic expressions for the cross section formulae [29] are too lengthy to be repeated here. We follow the same logic as in the sequel of (3.1) and (3.2). After integration over the momenta of the outgoing quarks and the gluon the result [9] takes the form illustrated in fig. 8: all diagrams can be drawn in such a way, that at the upper end we have the fermion-loop $D_{2,0}$, and the s -channel gluon is contained in an effective vertex function which is similar (but not identical) to the $2 \rightarrow 4$ gluon vertex in (2.19) (fig. 1b). From [9] we take the expression:

$$D_{q\bar{q}g,0}^{\ell,t}(\mathbf{l}, \mathbf{l}') \Big|_{t=0} = \frac{3g^2}{4\sqrt{2}} D_{2,0}^{\ell,t} \otimes \left\{ 2G(\mathbf{l}, -\mathbf{l}) + 2G(\mathbf{l}', -\mathbf{l}') + 2G(\mathbf{l}, \mathbf{l}') + 2G(\mathbf{l}, -\mathbf{l}') + \right. \\ \left. + G(\mathbf{l} + \mathbf{l}', -\mathbf{l} - \mathbf{l}') + G(\mathbf{l} - \mathbf{l}', -\mathbf{l} + \mathbf{l}') - 2G(\mathbf{l}, -\mathbf{l} + \mathbf{l}') \right. \\ \left. - 2G(\mathbf{l}, -\mathbf{l} - \mathbf{l}') - 2G(\mathbf{l}', \mathbf{l} - \mathbf{l}') - 2G(\mathbf{l}', -\mathbf{l} - \mathbf{l}') \right\}. \quad (3.15)$$

Here $G(\mathbf{a}, \mathbf{b})$ is the same function that enters into the convolution $D_2 \otimes V$ (eqns. (2.18), (2.19)). The ladders at the lower end of this vertex, again, denote (leading-twist) gluon structure functions (3.10).

Since we did not present the explicit formulae for the (unintegrated) diffractive cross sections, we only briefly sketch the qualitative picture (details can be found in [29]). Let \mathbf{k}_2 be the transverse momentum of the gluon, and $\mathbf{k}_1, -(\mathbf{k}_1 + \mathbf{k}_2)$ those of the quarks. The easiest way is to start with the hard region (i.e. the transverse momenta of quarks and gluons are large), and to consider configurations where the momenta are ordered: $k_2^2 < k_1^2$. In this region, the transverse cross sections goes as $d\sigma^t \sim 1/[k_1^2 k_2^4] \cdot [x_{\mathbb{P}} g(x_{\mathbb{P}}, k_2^2)]^2$ and the longitudinal cross section behaves as $d\sigma^\ell \sim 1/[k_1^4 k_2^4] \cdot [x_{\mathbb{P}} g(x_{\mathbb{P}}, k_2^2)]^2$. By dimensional counting, this region belongs to twist-four. Leading-twist can be obtained if one realizes that the integration over the gluon momentum \mathbf{k}_2 is dominated by the small momentum region, i.e. by nonperturbative physics. The remaining \mathbf{k}_1 -integral provides, for the transverse photon, a $\ln Q^2$ -enhancement, whereas for the longitudinal photon it does not (table 3).

The derivation of the twist-four contributions, now, follows the same way as for $q\bar{q}$ -production.

We use the (ω, ν) -representation for (3.15), and the twist-four part (near $\nu = -2$) takes, for the transverse photon, the form:

$$\frac{1}{\omega} D_{q\bar{q}g,0}^t(\omega, l^2, l'^2)^{\tau=4} = -a_2^t \frac{9}{\pi} \frac{1}{\omega} \sum_f e_f^2 \alpha_s^3 \frac{Q^2}{Q_0^2} \left\{ 2l^4 \ln l^2 + 2l'^4 \ln l'^2 - \left[2l^4 + 2l'^4 - 8l^2 l'^2 \right] \ln \left[\max(l^2, l'^2) \right] \right\}. \quad (3.16)$$

Similarly, for the longitudinal photon we obtain:

$$\frac{1}{\omega} D_{q\bar{q}g,0}^\ell(\omega, l^2, l'^2)^{\tau=4} = \frac{b_2^\ell}{2} \frac{9}{\pi} \frac{1}{\omega} \sum_f e_f^2 \alpha_s^3 \frac{Q^2}{Q_0^2} \left\{ 2l^4 \ln^2 l^2 + 2l'^4 \ln^2 l'^2 - \left[2l^4 + 2l'^4 - 8l^2 l'^2 \right] \ln^2 \left[\max(l^2, l'^2) \right] \right\}. \quad (3.17)$$

The integration over \mathbf{l}, \mathbf{l}' is done in the same way as described after (3.10). With (3.10) for the unintegrated structure function we find

$$\Delta \left. \frac{d\sigma^{q\bar{q}g,t}}{dt} \right|_{t=0} = -\frac{4\pi^2 \alpha_{\text{em}}}{Q^4} \frac{9a_2^t}{16\pi^3} \frac{\alpha_s^3}{2\gamma_2} \frac{1}{\omega} \sum_f e_f^2 \left\{ 1 - \exp \left(\frac{2\gamma_2}{\omega} \ln \frac{Q^2}{Q_0^2} \right) \right\} \varphi_2^2(\omega) \quad (3.18)$$

and

$$\Delta \left. \frac{d\sigma^{q\bar{q}g,\ell}}{dt} \right|_{t=0} = \frac{4\pi^2 \alpha_{\text{em}}}{Q^4} \frac{9b_2^\ell}{32\pi^3} \frac{\alpha_s^3}{2\gamma_2} \sum_f e_f^2 \left\{ \exp \left(\frac{2\gamma_2}{\omega} \ln \frac{Q^2}{Q_0^2} \right) - 1 - \frac{2\gamma_2}{\omega} \ln \frac{Q^2}{Q_0^2} \right\} \varphi_2^2(\omega) \quad (3.19)$$

for the transverse and for the longitudinal photon, resp. Finally, performing the integration over t and replacing φ_2^2 by $Q_0^2 \varphi_4^{\text{diff}}$ leads to our final expressions for the twist-four corrections to the diffractive structure functions $\Delta\sigma^{q\bar{q}g,t}$ and $\Delta\sigma^{q\bar{q}g,\ell}$.

An important feature of these results is the sign structure (summarized in table 3). For both the transverse and the longitudinal photon we find the opposite signs compared to $q\bar{q}$ -production (table 2). This implies that when we are calculating the total twist-four corrections to the diffractive cross section – either transverse or longitudinal – we are adding two terms ($q\bar{q}$ and $q\bar{q}g$) of opposite signs. Moreover, the higher-twist corrections for the transverse and for the longitudinal diffractive cross sections have opposite signs. This clearly allows for the possibility of substantial cancellations, in particular in the corrections to $F_2^{\text{D}} = F_\ell^{\text{D}} + F_t^{\text{D}}$. The longitudinal diffractive cross section may, therefore, be a cleaner place to look for twist-four corrections.

It is not difficult to generalize this discussion to the production of more gluons in the region of very small β . For example, for the (integrated) production cross section of two gluons we have to calculate the diagrams shown in fig. 9. As before, use has been made of eqns. (2.41) and (2.43). In this way all diagrams in fig. 9 can be rearranged in terms of the vertex (3.15), and they can be grouped into two classes. Beginning with the fermion-loop at the top of the diagram, we have, in the case of fig. 9a, one BFKL rung, then the vertex (3.15), and further below the two-gluon ladders for the unintegrated gluon structure functions. In case of fig. 9b, there is no rung between the fermion-loop and the vertex (3.15), but instead four possible rungs below the vertex at the top of the gluon ladders. Similarly, for three gluons we have three possibilities: two gluon rungs above the vertex, one rung above and one set of rungs below, or two sets of rungs below.

3.4 Connection with the Structure Functions $F_{\ell,t}$ and the AGK Cutting Rules

After we have discussed the different diffractive cross sections, we, now, turn to the question of how these contributions enter into the inclusive cross section (2.17). An important ingredient are the AGK cutting rules [14].

We first return to the total cross section (2.17) and recapitulate how the AGK rules work. Let us, for the moment, replace the proton by a virtual photon, i.e. we consider the elastic scattering of a virtual photon on another virtual photon. This process can be treated perturbatively. For the time being we do not expand in powers of Q_0^2/Q^2 , but consider the Regge limit at large but finite Q^2 . In order to study the AGK rules, we start with the discontinuity across the four-gluon t -channel intermediate state. Disregarding all unnecessary details, this discontinuity takes the form

$$\text{disc}_\omega F_{\gamma^*\gamma^*} \sim \frac{1}{4!} C_4^* \otimes C_4 \quad (3.20)$$

where $F_{\gamma^*\gamma^*}$ denotes the t -channel partial wave for the $\gamma^*\gamma^*$ scattering process, $C_4(k_1, k_2, k_3, k_4; \omega) = (\omega - \sum \beta(k_i)) D_4(k_1, k_2, k_3, k_4; \omega)$ is the amputated $\gamma^*\gamma^* \rightarrow 4$ -gluons partial wave, and the symbol \otimes contains all phase space factors. For C_4 we have the same decomposition (eqn. (2.16)) as for D_4 . In particular, C_4^I is completely symmetric, and C_4^R contains a symmetric piece and a piece with mixed symmetry (cf. the discussion after (2.41)). In the unitarity integral (3.20), we take from both C_4 and C_4^* either the symmetric pieces or the pieces with mixed symmetry, i.e. there is no interference term.

First consider the symmetric pieces, e.g. C_4^I for both factors in (3.20). Writing C_4^I in terms of the auxiliary potentials $T_{(ij)(kl)}$ from our discussion above, we have in our unitarity integral on the r.h.s. of (3.20) the three identical ‘diagonal’ terms $T_{(12)(34)} \otimes T_{(12)(34)}$, $T_{(13)(24)} \otimes T_{(13)(24)}$, and $T_{(14)(23)} \otimes T_{(14)(23)}$. Together with the statistical factor $1/4!$, this gives a weight factor $1/2(1/2)^2$ for the diagonal term (this counting does not include color). Similarly, ‘nondiagonal’ terms, $T_{(12)(34)} \otimes T_{(13)(24)}$ etc., yield the weight factor $(1/2)^2$. In order to verify the AGK cutting rules we compare $2 \text{Im} T_{\gamma^*\gamma^*}$ of this amplitude with the different cuts, σ_0 , σ_1 , and σ_2 (the subscripts refer to the number of cut ladders). The (diagonal) ‘diffractive cut’ σ_0 has the cutting line between the gluon lines ‘2’ and ‘3’. Its contribution is positive and has the weight $(1/2)^2$ (due to the statistical factors inside the ladders). For the ‘double multiperipheral’ cut σ_2 the cutting line runs also between gluons ‘2’ and ‘3’, but its (positive) contribution has the weight $2(1/2)^2$. Finally, the ‘absorptive cut’ σ_1 is negative; the cutting line runs between line ‘1’ and ‘2’ or ‘3’ and ‘4’, and the counting gives $-2 \cdot 3 \cdot 1/3! = -1$. Adding all these contributions, we arrive at $-(1/2)^2$, i.e. minus the diffractive cross section σ_1 . The result agrees with $2 \text{Im} T_{\gamma^*\gamma^*}$, as anticipated by the AGK rules. Two features of these results are important for us: in total, the four-gluon t -channel state gives a *negative* correction to the single-ladder contribution (this justifies the minus sign in (2.17)), and its absolute value equals the ‘diffractive cut’ σ_0 . It is easy to verify that the same conclusion also holds for nondiagonal pieces $T_{(12)(34)} \otimes T_{(13)(24)}$ etc.

Next, the part with mixed symmetry: in (3.20) we put C_4^R for both C_4 -factors, and we take the terms with the anti-symmetric structure constants ($f^{abc'} f^{c'cd}$ etc.). Their color and momentum structure is the same as in (2.33). They are connected with the odd signature reggeized gluon. Again, in the unitarity integral we have diagonal terms of the type $f_A(12, 34) \otimes f_A(12, 34)$. Their total weight is $2(1/2)^2$. In the counting of the nondiagonal terms we encounter several cancellations: the weight factor turns out to be $1/2$. Now, we compare this with the cuts σ_0 , σ_1 , and σ_2 . For the

diagonal σ_0 and σ_2 contributions where the cutting line runs between gluon ‘2’ and ‘3’, we find the weight factors $(1/2)^2$ and $2(1/2)^2$, resp. They are the same as the counting factors for the even signature ladders which we have discussed before. In particular, we again have the negative sign for the sum of the three cuts. There is, however, an important difference between even and odd signature reggeons: for odd signature the real part of the signature dominates, and the leading contribution σ_0 is contained in the LO BFKL equation. The only contribution to σ_0 from the four-gluon intermediate state comes from the ‘diagonal’ pieces which present the two gluon contributions to the gluon trajectory functions. Consistency, therefore, requires that the magnitude of this term is linked to the leading order BFKL ladder. One can check from (2.41) that this condition is, indeed, satisfied.

In summary, the AGK rules allow us to determine the sign of our initial conditions. We return to deep inelastic scattering off the proton, consider the twist-four term in the expansion in powers of Q_0^2/Q^2 and replace, in (3.20), the second C_4 factor by our general ansatz (2.31), i.e. by our nonperturbative initial conditions φ_{4S} and φ_{4A} . In order to preserve the sign structure dictated by the AGK rules, both functions have to be positive. Moreover, since φ_{4A} is connected with the reggeization of the gluon trajectory function, it is linked to the size of the twist-four part in the BFKL ladder, $\Delta F^{(2)}$. In this first attempt to estimate the higher-twist contribution, we will consider two different values for φ_{4A} which we expect to present a reasonable range.

Next we attempt to relate these unknown initial conditions to the diffractive $q\bar{q}$ cross section (3.13), in order to obtain an estimate of their magnitude. The easiest way is a comparison of the two-ladder diagrams in $\Delta F^{(4)}$ with the diffractive cross section (fig. 6). We use the coupling (2.31), take the color singlet states of the two ladders, project onto the twist-four term and compute the ‘diffractive’ cut σ_0 between the gluon lines 2 and 3. Equating the result with the cross section 3.13 we arrive at the equation:

$$\frac{5}{4}\varphi_{4S} - \frac{3}{4}\varphi_{4A} = \varphi_4^{\text{diff}}. \quad (3.21)$$

This result is quite remarkable, since – at first sight – it does not seem to agree with the AGK rules. Namely, naively one might have expected that $\varphi_{4S} = \varphi_4^{\text{diff}}$, i.e. the four-gluon contribution equals (up to the overall minus sign which we have extracted already in (2.17)) the diffractive cross section. Let us recapitulate the origin of the l.h.s. of (3.21): from (2.16) we deduced that QCD diagrams for $T_{\gamma^*\gamma^*}$ with four gluons in the t -channel have to be decomposed according to their symmetry under permutation of color and momenta (the antisymmetric terms have their origin in the reggeization of the gluon). The same argument forces us to use the ansatz (2.31)-(2.33), i.e. we have the two functions φ_{4S} and φ_{4A} . The AGK rules work for each term separately, but the t -channel state with four reggeized gluons couples only to φ_{4S} . Finally, when computing the two-ladder diagrams in $T_{\gamma^*\gamma^*}$, we find for the coupling of two ladders to the proton the combination on the l.h.s. of (3.21) (the fact that the factor in front of φ_{4S} equals 5/4 and not 1 is a result of the presence of the second and third term in (2.32)).

There are two important consequences of (3.21). First, from this single condition we cannot fix both initial conditions φ_{4S} and φ_{4A} . Secondly, due to the minus sign on the l.h.s., φ_{4S} can be larger than the ‘naive’ expectation $\varphi_{4S} = \varphi_4^{\text{diff}}$. We propose to proceed as follows. The longitudinal cross section for diffractive $q\bar{q}$ -production allows to estimate φ_4^{diff} . From our discussion above we know that φ_{4A} is connected with the reggeization of the gluon: in our numerical analysis we will vary φ_{4A} in such a way that its correction to the leading-twist structure function ranges between 20 %

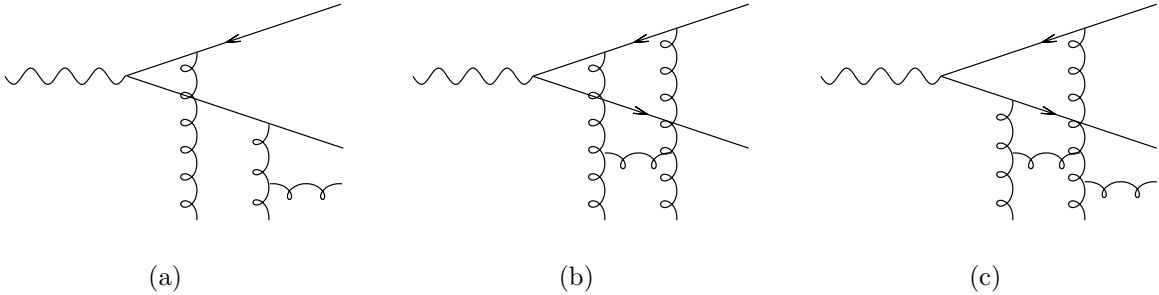


FIG. 10: Three sample diagrams which contribute to D_4 at order α_s^3 ((a) and (b)) and at order α_s^4 (c). Diagrams (a) and (c) enter also into diffractive $q\bar{q}g$ -production at leading and next-to-leading order, resp. For the diffractive process the two t -channel gluons must certainly be in the color singlet, while there are also contributions from other color states which enter into D_4 .

and 100 % (see below). Together with the variation of φ_{4A} we also find a change in the strength of φ_{4S} and ΔF^I , the most interesting higher-twist contribution in the small x region.

3.5 The Sign Structure

It may be helpful to briefly recapitulate the sequence of our arguments, in particular the sign structure. The easiest way is to start with the twist-four corrections to the diffractive cross sections; their signs are summarized in tables 2 and 3. Starting with $q\bar{q}$ -production, in the transverse case twist-four is a correction to leading-twist and has a negative sign. The longitudinal cross section starts with twist-four and is positive. Next diffractive $q\bar{q}g$ -production: all signs change, compared to $q\bar{q}$ -production. This is due to the vertex (3.15) which has an intrinsic minus sign.

In the next step we have argued that when generalizing to an arbitrary number of gluons in the diffractive final state and allowing for evolution in the unintegrated gluon structure function we generate all diagrams contained in $\Delta F^{(4)}$: although there is no direct correspondence between the splitting $\Delta F^{(4)} = \Delta F^R + \Delta F^I$ and the different diffractive final states. As a memo we nevertheless can say that ΔF^R “is related to” (i.e. gets the same sign as) the cross section for $q\bar{q}$ -production, and a similar correspondence holds for ΔF^I and diffractive $q\bar{q}g$ -, $q\bar{q}gg$ -, ... -production.

In the last step we have to remember that it is not only the diffractive states which contribute to the structure functions. Making use of the AGK rules we conclude that taking into account all other energy discontinuities simply means changing the sign of the (total) diffractive contributions. The results are summarized in table 4.

4 Numerical Results

4.1 General Procedure and Determination of Initial Parton Distributions

Using the framework outlined above we have performed a numerical analysis. The first step to be discussed is how we fix the free parameters in the various initial distributions φ . From our

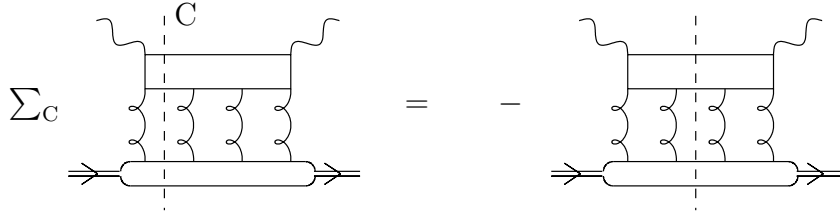


FIG. 11: The AGK rules: The sum over the three cuts, which is necessary for the computation of the inclusive structure function, gives a contribution that is equal to minus one times the term where only the diffractive cut is applied.

discussion it should have become clear that we have to determine four initial distributions, viz. φ_2 for $\Delta F^{(2)}$, φ_3 for the three-gluon correction to $\Delta F^{(2)}$, and φ_4 which couples to both ΔF^R and ΔF^I . Moreover, φ_4 consists of a symmetric part and a part with mixed symmetry, cf. eqn. (2.31). All initial distributions depend on ω , and a pole at some positive ω -value corresponds to a rising (in $1/x$) initial condition.

Let us begin with a detailed discussion of the four-gluon case. As indicated before, we relate φ_4 directly to the longitudinal diffractive $q\bar{q}$ cross section (eqs. (3.13) and (3.21)), and the latter can be estimated with the help of the measured cross section of longitudinal vector production if we sum over all vector mesons in the final state [28]. Let us assume that – after integration over t , p_t^2 and M^2 , and including diffractive dissociation of the proton – this cross section reaches a few per cent of the inclusive (transverse) leading-twist cross section at $x = 10^{-3}$, $Q^2 = 10 \text{ GeV}^2$. Using this estimate we fix the initial condition φ_4^{diff} and, with the help of (3.21), also the combination of the initial conditions φ_{4S} and φ_{4A} , which enter into the four-gluon amplitude. Since this procedure fixes only the difference $5\varphi_{4S} - 3\varphi_{4A}$ (cf. (3.21)) we still have freedom for determining the ratio of φ_{4S} and φ_{4A} . In a perturbative toy model, namely deep inelastic scattering off a virtual photon, φ_{4A} is linked to the leading-twist amplitude: it provides the t -channel four-gluon state inside the BFKL amplitude (cf. the discussion in section 3.4) and, hence, can be derived from the size of the leading-twist contribution. However, when replacing the (target) virtual photon by the proton, this connection becomes somewhat uncertain, and we, therefore, consider different values for the ratio $\varphi_{4A}/\varphi_{4S}$. Starting with the toy model, we find it reasonable to expect that φ_{4A} should not be smaller than φ_{4S} . We, therefore, set $\varphi_{4A} = \lambda\varphi_{4S}$ and consider the range $1.0 < \lambda < 1.5$. Eqn. (3.21) indicates that this seemingly small variation will nevertheless have a large effect: if λ reaches the vicinity of $5/3 \approx 1.6$, φ_{4S} increases strongly (for fixed φ_4^{diff}). This enhances the contribution of ΔF^I , whereas ΔF^R changes much less, since it depends on both, φ_{4S} and φ_{4A} (cf. (2.42)). Since ΔF^I and ΔF^R enter with different signs, a variation of λ between 1 and 1.5 will have a large effect on the total twist-four contribution.

Having fixed the initial conditions φ_4 we can, in principle, predict other higher-twist corrections to the diffractive cross section. In a future analysis of diffractive jet data at HERA it may be possible to measure the twist-four $q\bar{q}$ and $q\bar{q}g$ contributions directly; this will provide an important consistency check of this strategy. As we have said before, because of the cancellations between the $q\bar{q}$ and $q\bar{q}g$ parts the total higher-twist contribution to F_2^D may be smaller than the naive estimate based on longitudinal $q\bar{q}$ production.

As to the other two initial conditions, φ_2 and φ_3 , we have not been able to relate them to any direct

	$F_2^{\tau=2}$	$\Delta F^{(2)}$	$\Delta F^{(3)}$	ΔF^{R}	ΔF^{I}
long.	+	-	+	-	+
trans.	+	+	-	+	-

TABLE 4: The various contributions to F_2 enter with different signs.

measurement. Starting with φ_2 , for simplicity we assume that at the scale Q_0^2 the initial distribution for twist-four is the same as for the leading-twist case. It follows that the transverse contribution is positive, whereas the longitudinal twist-four part of the two-gluon amplitude contributes with a negative sign to F_2 , since b_2^ℓ in eqn. (2.14) is negative. For the three-gluon amplitude we make an even more ad hoc choice and demand that at $x = 10^{-3}$, $Q^2 = 1 \text{ GeV}^2$ its absolute magnitude in ΔF_ℓ equals the mean value of $\Delta F^{(2)}$ and ΔF^{R} . Our numerical analysis shows that the choice of the point, $x = 10^{-3}$, $Q^2 = 1 \text{ GeV}^2$, hardly influences our results, since $\Delta F^{(2)}$, $\Delta F^{(3)}$ and ΔF^{R} have nearly the same shape (up to factors $\sqrt{\alpha_s(Q^2)}$ and $\alpha_s(Q^2)$). In principle, for both, $\varphi_2^{\tau=4}$ and the three-gluon term φ_3 , not only the absolute magnitude but also the overall signs are undetermined. We have fixed these signs with the help of the following considerations. First, in $\Delta F^{(2)}$ there is no reason why there should be a sign change when going from leading-twist to twist-four. As an example, in our toy model described above, deep inelastic scattering of two virtual photons with virtualities $Q_1^2 \ll Q_2^2$, both leading- and higher-twist have the same sign. Next, as we have argued above, $\Delta F^{(3)}$ and ΔF^{R} are supposed to be related to the NLO and NNLO corrections to BFKL. Our choice of signs is consistent with the expectation that these corrections have alternating signs, i.e. $\Delta F^{(3)}$ is negative with respect to $\Delta F^{(2)}$, and ΔF^{R} is positive again. The sign of ΔF^{R} , on the other hand, has to be consistent with (2.42) and the AGK cutting rules, i.e. positive for the transverse part. All in all we, therefore, believe that our choice of signs is on a rather safe ground. Table 4 summarizes the sign structure of the various leading- and next-to-leading twist parts in F_2 , cf. (1.1).

As one of the results of our analysis we observe that ΔF^{R} and ΔF^{I} enter with opposite signs and, depending on the choice of parameters, tend to weaken each other: although we have some freedom for determining the relative contribution of $\varphi_{4\text{S}}$ and $\varphi_{4\text{A}}$, both, ΔF^{R} and ΔF^{I} , are sizeable and enter with opposite signs. But despite these cancellations the total twist-four contribution is not small at $Q^2 = 1 \text{ GeV}^2$. It is negative, and the contribution of the transverse photon is substantially larger than that of the longitudinal one.

In our numerical analysis we have used our formulae in order to perform, in the kinematical regime of HERA, a “semiquantitative” numerical study of the potential rôle of twist-four at small x and low Q^2 . As we have emphasized several times the limitations due to the DLA are severe. On the leading-twist level it is known that this approximation, which in the anomalous dimension retains only the most singular (near $\omega = 0$) term, is insufficient to describe HERA data at small x and low Q^2 : it is, at least, necessary to keep also the constant term within the gluon anomalous dimension. We, therefore, expect that a similar level of accuracy will be needed also for a realistic estimation of twist-four corrections. In order to minimize the inaccuracy we present the ratios of the twist-four contributions to the DLA leading-twist transverse structure function. In this way we hope that our results describe the trend correctly on a semiquantitative level. For leading-twist we are fixing the free parameter within the initial distribution by demanding that at $x = 10^{-3}$, $Q^2 = 10 \text{ GeV}^2$ our DLA expression for F_2 is equal to the corresponding MRRS [33] value.

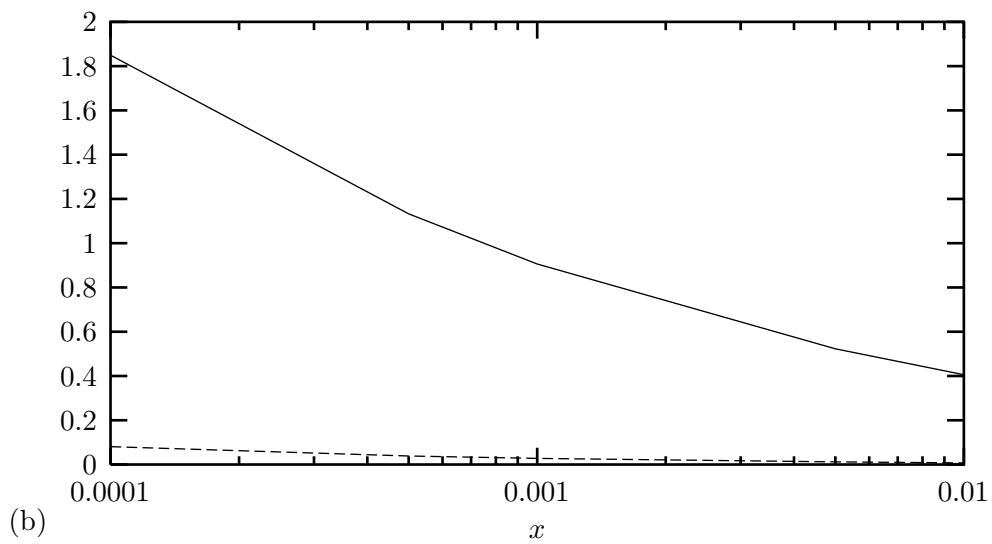
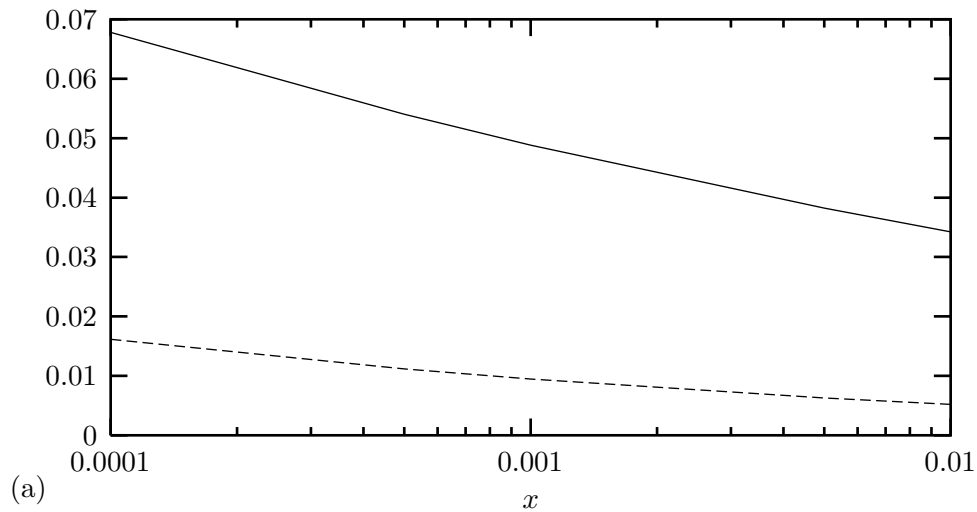


FIG. 12: Transverse leading-twist structure function in DLA (solid line) in comparison with the longitudinal twist-four contribution to F_2 of the diffractive $q\bar{q}$ -production process as a function of x at (a) $Q^2 = 1 \text{ GeV}^2$ and (b) $Q^2 = 10 \text{ GeV}^2$. For this scenario, we have chosen constant initial distributions at $Q_0^2 = 0.5 \text{ GeV}^2$.

As outlined above, we are using the diffractive vector production cross section to estimate twist-four contributions to F_2 . To be precise, we assume that the longitudinal twist-four $q\bar{q}$ cross section (3.13) reaches three per cent at $Q^2 = 10 \text{ GeV}^2$, $x = 10^{-3}$ relative to the transverse leading-twist contribution. As to the choice of the starting scale Q_0^2 , our limitations due to the DLA are causing a particular problem. In DLA, the four-gluon amplitude ΔF^I vanishes at $Q^2 = Q_0^2$, and it needs some Q^2 evolution before it “forgets” about its starting condition. In an analysis which goes beyond the DLA, we would start with some nonzero value. In order to escape from this unrealistic behavior near Q_0^2 , we have chosen a very small value for the input scale, viz. $Q_0^2 = 0.5 \text{ GeV}^2$, and hope that for Q^2 values greater than, say, 0.8 GeV^2 , these unwanted effects are suppressed. For the computation of the double Mellin transforms we have used the method outlined in ref. [34], which proves to be very accurate and efficient. The numerical results of our analysis also strongly depend upon the x -shape of the initial distributions, both for the leading-twist and for the twist-four correction. We, therefore, compare three different scenarios, two with constant initial conditions and with different choices for the ratio $\varphi_{4A}/\varphi_{4S}$, and one with rising initial conditions.

4.2 Constant Initial Parton Distribution

Following a presently popular trend in analysing HERA data, we first assume that the leading-twist gluon structure function at the input scale Q_0^2 is flat at small x . In two subsections we will consider the results for two different choices of the ratio $\lambda \equiv \varphi_{4A}/\varphi_{4S}$, viz. $\lambda = 1$ and $\lambda = 1.5$. First, we show in figs. 12a and 12b the x -dependence of the transverse leading-twist structure function in comparison with the twist-four contribution due to diffractive longitudinal $q\bar{q}$ -production. In the lower figure the point $x = 10^{-3}$ is our point of comparison: the higher-twist term has reached 3% of F_2 . The comparison of the two figures shows the expected behavior: higher-twist becomes more important at low Q^2 . If there would be only this twist-four contribution, we would have a positive 20% correction at $Q^2 = 1 \text{ GeV}^2$.

4.2.1 Weak Anti-Symmetric Initial Distribution ($\lambda = 1$)

The picture changes quite substantially if we include the other twist-four contributions. We start with a discussion of the longitudinal part. Fig. 13a shows how this twist-four part is composed of the four contributions (the twist-four part of the two-gluon amplitude $\Delta F^{(2)}$, $\Delta F^{(3)}$ and the four-gluon contributions, ΔF^R and ΔF^I) at $Q^2 = 1 \text{ GeV}^2$. In order to simplify comparisons, we have normalized all twist-four contributions to the corresponding DLA transverse leading-twist values. As can be seen, two of the four contributions ($\Delta F^{(3)}$ and ΔF^I) enter with positive and the remaining two with negative signs, so that the sum (solid line) gives a very small contribution. Let us take a closer look at the cancellations, in particular those between ΔF^R and ΔF^I . As we argued before, after we have set $\varphi_{4A} = \varphi_{4S}$, the relative sign as well as the relative magnitude are fixed: in fig. 13a (at $Q^2 = 1 \text{ GeV}^2$) ΔF^R and ΔF^I almost compensate each other. Due to (2.45) ΔF^I will become dominating at very small x . In our calculations this region is not yet reached.

The sign pattern of the individual contributions does not change when we go to higher Q^2 -values (fig. 13b), although the total sum, now, becomes positive in the full x -interval. A look at the absolute values, which are not shown here, tells us that the twist-four contributions have actually increased compared to the case at $Q^2 = 1 \text{ GeV}^2$ – the $1/Q^2$ suppression sets in rather late. But

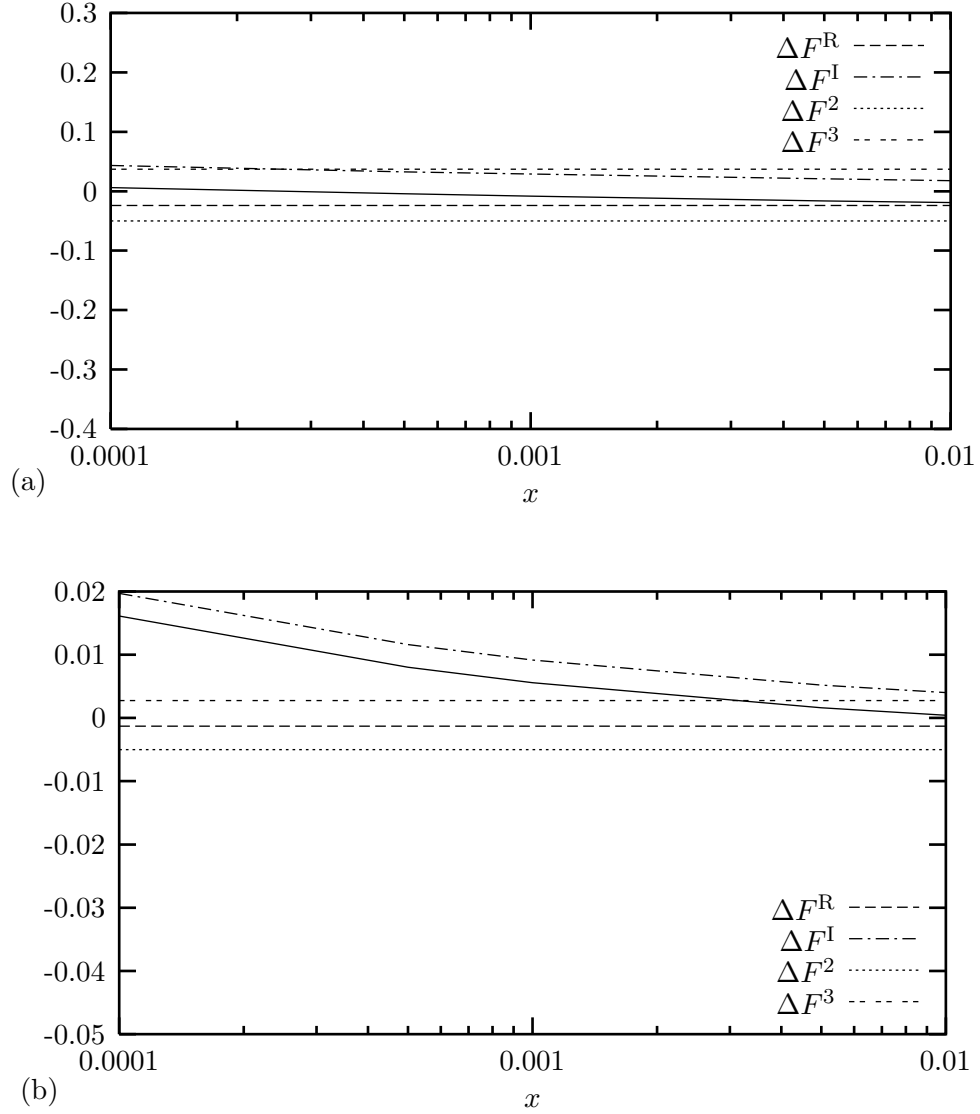


FIG. 13: Longitudinal part of the twist-four contributions (solid line) and the four terms they are composed of as a function of x at (a) $Q^2 = 1 \text{ GeV}^2$ and (b) $Q^2 = 10 \text{ GeV}^2$. Normalization with transverse leading-twist values.

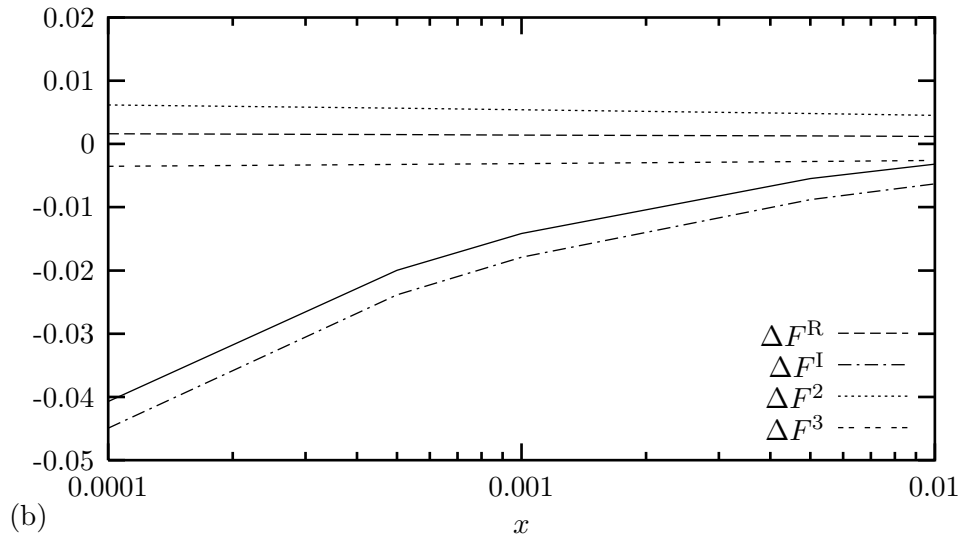
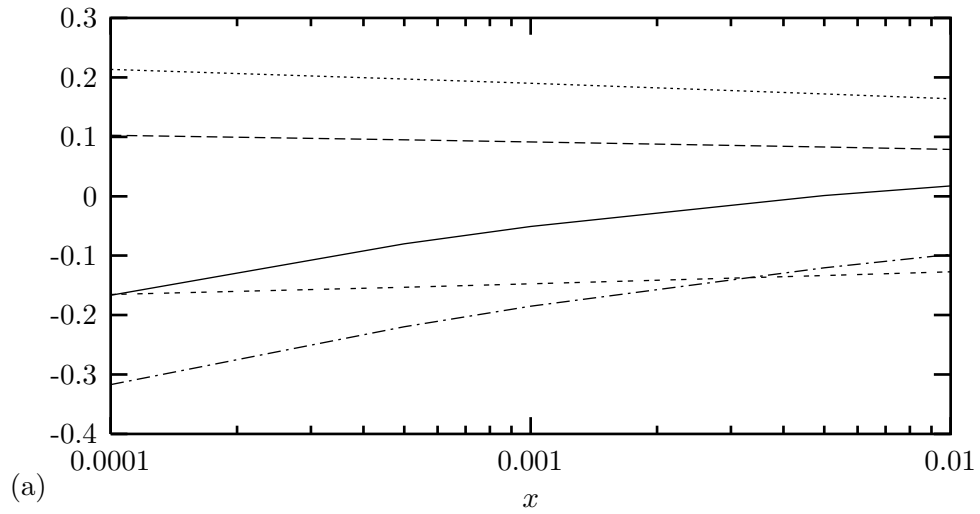


FIG. 14: Same as in fig. 13 but, now, for the transverse twist-four contributions.

since leading-twist has increased as well, the ratio of the two decreases. Moreover, since ΔF^1 is the twist-four contribution with the strongest evolution (cf. (2.45)) the total twist-four contribution is positive and reaches up to 1.5% of leading-twist (fig. 13b). As to the other pair of contributions ($\Delta F^{(2)}$ and $\Delta F^{(3)}$), they also come with opposite signs and, approximately, the same strength. But this clearly depends very much on our choice of the initial conditions. For example, a smaller choice of φ_3 , the initial distribution of the three-gluon amplitude, which, as outlined in section 4.1, cannot be related to any experimental measurement, results in significant smaller values of ΔF_ℓ .

Next we take a look at the transverse contributions (fig. 14). As always in our discussion, this contribution represents the DLA, and as we discussed before, it is suppressed by one power of $\ln(Q^2/Q_0^2)$ in comparison to the longitudinal (twist-four) photon. Nevertheless, our results for ΔF_t represent the leading contributions for the transverse structure function. We plot our results in the same way as we did for the longitudinal case, and the x distributions for the two values $Q^2 = 1 \text{ GeV}^2$ and $Q^2 = 10 \text{ GeV}^2$ are shown in figs. 14a and b, resp. First, one notices that for each separate twist-four contribution (again normalized to the leading-twist term) the transition from $Q^2 = 1 \text{ GeV}^2$ to $Q^2 = 10 \text{ GeV}^2$ results in a much stronger decrease than in the longitudinal case. This is certainly due to the absence of the $\ln Q^2$ -factor, which makes the Q^2 -evolution weaker. Altogether, at $Q^2 = 1 \text{ GeV}^2$ the transverse twist-four terms, which enter into the correction to F_t are of much larger size than in the longitudinal case and the sum of all four terms, now, gives a negative contribution.

In our scenario the transverse twist-four contribution (fig. 14a) gives a negative correction which at $Q^2 = 1 \text{ GeV}^2$ and $x = 10^{-4}$ reaches 15% of the leading-twist. The main reason for this is that ΔF^1 is the dominating contribution. If we would go to even smaller values of x the dominance of ΔF^1 would become even more pronounced but one has to keep in mind that in this case even higher-twist contributions (twist-six, etc.) will, very likely, become important, as well. At $Q^2 = 10 \text{ GeV}^2$ (fig. 14b) the transverse twist-four contribution has gone down to less than 4%. Compared to the longitudinal case, the twist-four corrections of the transverse photon clearly dominates, and we expect that this remains true even if we go beyond the DLA. We can use our numerical results to determine the contribution of φ_{4A} within ΔF^R : using (2.42) and the numerical values in fig. 14 we deduce that (for the transverse photon at $Q^2 = 1 \text{ GeV}^2$) it reaches about 20% of leading-twist. We believe that this is a rather low value. In order to further decrease φ_{4A} , we would have to choose $\lambda < 1$. This seems to be rather unlikely if we can believe the results of our toy model.

Finally, figs. 15a and b show the Q^2 -dependence of the longitudinal and transverse twist-four contributions at $x = 10^{-3}$. As a general feature, we observe the interplay between the $1/Q^2$ suppression factor and the rise in the Q^2 -evolution. In both figures, the change of the sign in the sum of all contributions is due to the increase of ΔF^1 . Since we have performed our computations in DLA, the various twist-four contributions either vanish for $Q^2 \rightarrow Q_0^2$ or become a small constant. Moreover, ΔF^1 goes much faster to zero than all other contributions. As discussed before, this is a special problem of the DLA approximation of ΔF^1 . If we would take into account also sub-leading terms, this decrease of ΔF^1 for low Q^2 would be less distinct. It is, therefore, likely that the dominance of ΔF^1 in the twist-four corrections to F_2 is, in fact, stronger than found in our DLA analysis.

In summary, in this scenario the transverse twist-four contribution gives a negative correction of up to fifteen per cent of leading-twist at $Q^2 = 1 \text{ GeV}^2$, while the longitudinal twist-four contribution remains much smaller. In both cases we find cancellations between the various twist-four contributions which enter with different signs. In particular, ΔF^R contributes with a rather large amount

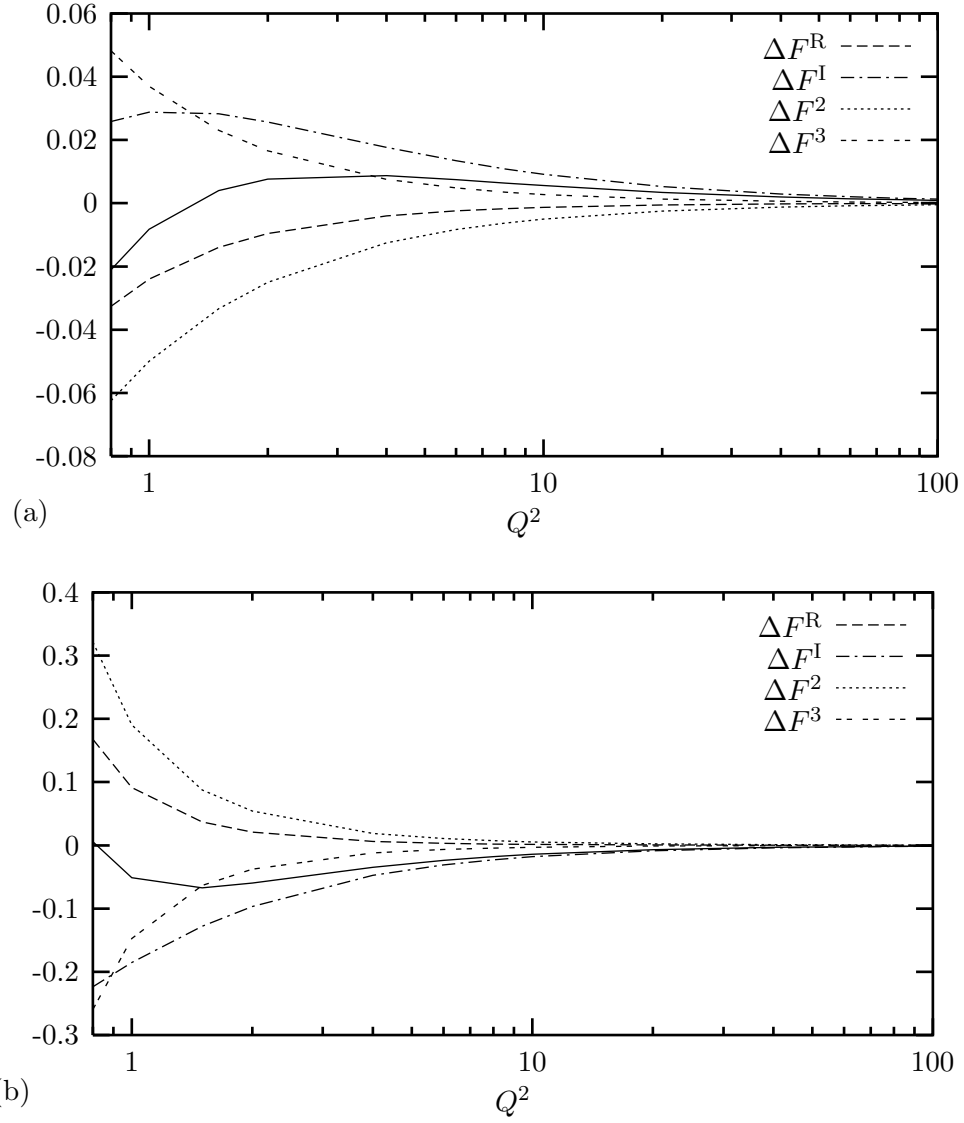


FIG. 15: Q^2 -dependence of the (a) longitudinal and (b) transverse twist-four contributions (solid line) and the four terms they are composed of at $x = 10^{-3}$. Normalization with transverse leading-twist values.

compared to ΔF^{I} . In retrospect it seems justified that we have taken into account also the twist-four contributions of $\Delta F^{(2)}$ and $\Delta F^{(3)}$. If we argue that $\Delta F^{(3)}$ should be related to the next-to-leading order corrections of the BFKL amplitude, ΔF^{R} would correspond even to NNLO corrections, while ΔF^{I} is the first term which contributes with a stronger power-behavior (cf. eqn. (2.45)).

4.2.2 Strong Anti-Symmetric Initial Distribution ($\lambda = 1.5$)

In this subsection we choose a stronger value for the initial condition $\varphi_{4\text{A}}$, viz. $\varphi_{4\text{A}} = 1.5 \varphi_{4\text{S}}$. Since φ_4^{diff} remains unchanged, our new scenario results in larger values for both $\varphi_{4\text{S}}$ and $\varphi_{4\text{A}}$, cf. (3.21). As we have outlined above, ΔF^{I} couples only to $\varphi_{4\text{S}}$, while ΔF^{R} couples to both $\varphi_{4\text{S}}$ and $\varphi_{4\text{A}}$. From (2.42) we expect that an increase in $\varphi_{4\text{A}}$ leads to a larger value of ΔF^{I} , while ΔF^{R} decreases. This is confirmed by the numerical values shown in fig. 16 for the longitudinal and transverse contributions at $Q^2 = 1 \text{ GeV}^2$. Both, in the longitudinal and in the transverse case, ΔF^{I} now dominates. The negative transverse twist-four correction has now gone up to more than 100% (at $x = 10^{-4}$) of the leading-twist contribution, whereas the positive longitudinal term reaches 15%. Certainly, if this scenario is realistic, our consideration of twist-four is not sufficient. As soon as twist-four reaches, say, fifty per cent of leading-twist, we have to consider also contributions with twist larger than four. Using, again, (2.42) we deduce that in this scenario (for the transverse photon at $Q^2 = 1 \text{ GeV}^2$) the contribution due to $\varphi_{4\text{A}}$ reaches about 130% of leading-twist, i.e. $\lambda = 1.5$ is likely to present an upper limit of $\varphi_{4\text{A}}$.

In both scenarios, considered so far, we find sizeable negative twist-four corrections at Q^2 near 1 GeV^2 : this confirms the expectation that the transition from the parton picture to Regge physics at $Q^2 = 0$ is indeed accompanied by sizable higher-twist. In particular, twist-four is negative at small x .

We believe that the largest uncertainties in this analysis are due to the unknown initial condition $\varphi_{4\text{A}}$. As we have demonstrated, a rather small variation in the ratio $\varphi_{4\text{A}}/\varphi_{4\text{S}}$ has a large effect on the relative contributions of ΔF^{I} and ΔF^{R} , and, therefore, on the total twist-four contributions. It is, therefore, important to find further restrictions on the size of $\varphi_{4\text{A}}$. Other sources of possible errors are our choice of the size of $\Delta F^{(3)}$, and the double logarithmic approximation. Moreover, as outlined above, it seems possible that ΔF^{I} at very low Q^2 would even be larger if one would take into account also sub-leading terms.

4.3 Increasing Initial Parton Distribution

As an alternative, we have considered a scenario with an initial gluon distribution which increases at small x : $xg(x, Q_0^2) \sim (1/x)^{\omega_0}$. For the twist-four part of the two-gluon amplitude and for the three-gluon contribution we assume the same power-behavior of the initial contribution as in the leading-twist case, and we have set $\omega_0 = 0.2$. As to the $\Delta F^{(4)}$ contributions, the situation is slightly more subtle. Since the four-gluon operator in ΔF^{I} is closely related to the double-exchange of DGLAP ladders, it seems reasonable to assume that the initial distribution of the four-gluon amplitude behaves like $(1/x)^{2\omega_0}$, i.e. the functions $\varphi_4(\omega)$ in (2.31) are assumed to have a pole at $2\omega_0$. For ΔF^{R} there is an ambiguity: on the one hand, the lowest order diagram is the four-gluon exchange, i.e. the evolution should start with φ_4 which rises as $\sim (1/x)^{2\omega_0}$. On the other hand, if we consider ΔF^{R} as a NNLO correction to the two-gluon operator (2.2), one might

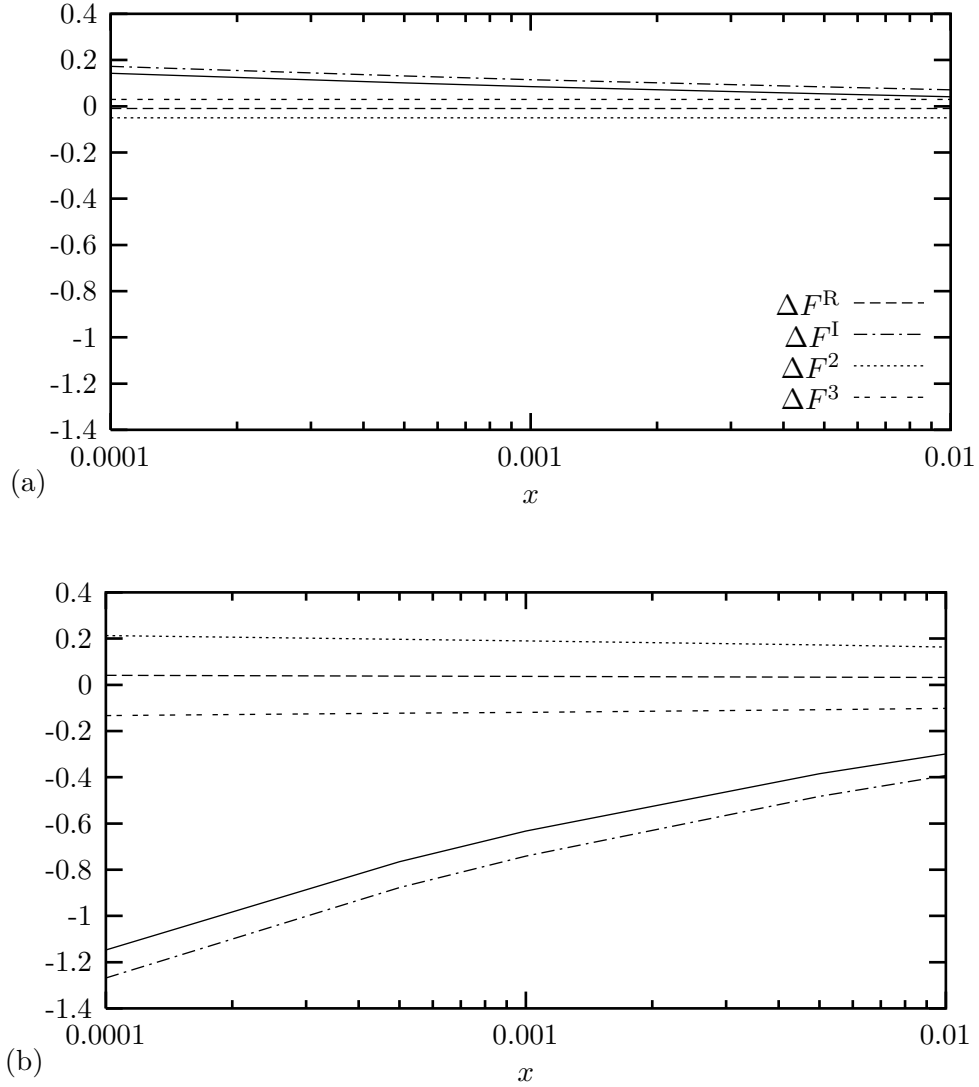


FIG. 16: (a) longitudinal and (b) transverse twist-four contributions as a function of x at $Q^2 = 1 \text{ GeV}^2$. For this scenario, we have chosen constant initial distributions with a strong choice of the anti-symmetric initial distribution that enters into $\Delta F^{(4)}$. The two diagrams, shown here, correspond to diagrams 13a and 14a in the previous scenario. Normalization with transverse leading-twist values.

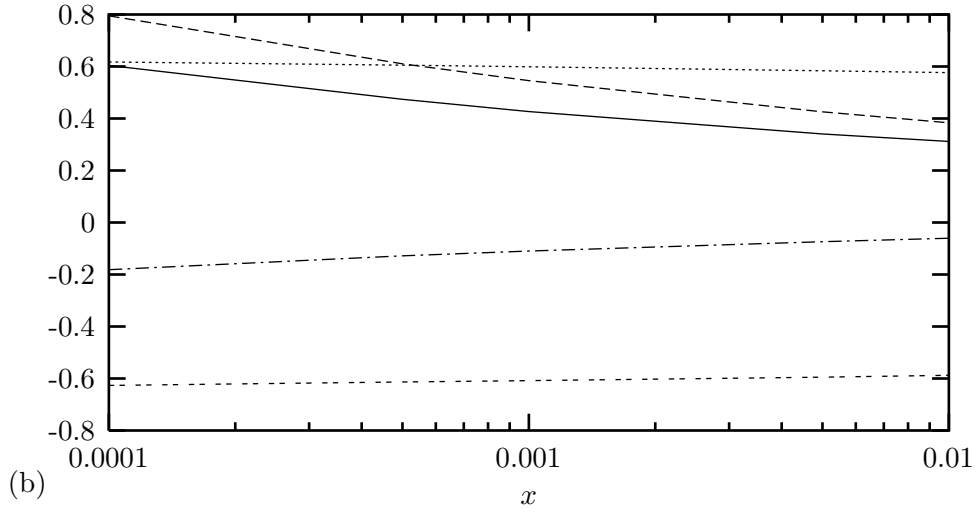
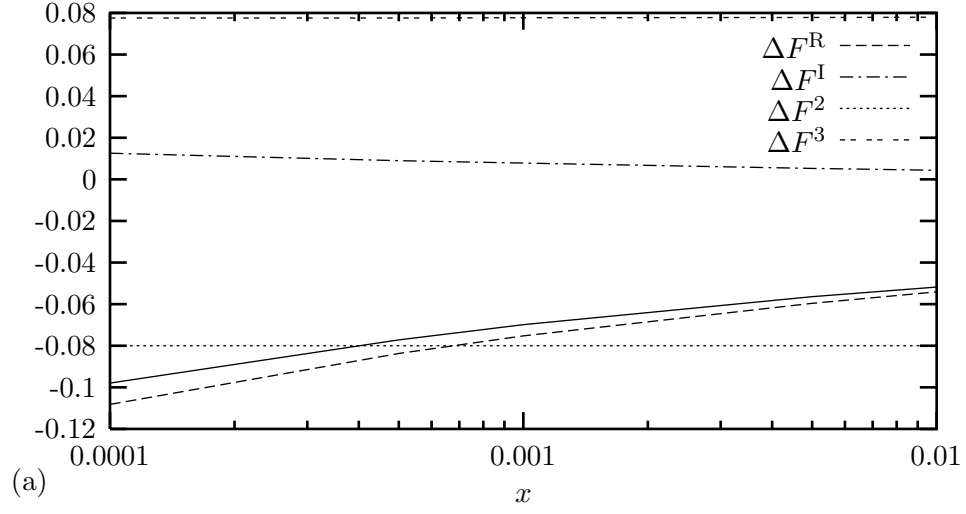


FIG. 17: (a) longitudinal and (b) transverse twist-four contributions as a function of x at $Q^2 = 1 \text{ GeV}^2$. For this scenario, we have chosen increasing initial distributions ($\omega_0 = 0.2$) at $Q_0^2 = 0.8 \text{ GeV}^2$. Normalization with transverse leading-twist values.

argue that we should have the same initial conditions as for the twist-four part of the two-gluon amplitude, i.e. $\sim (1/x)^{\omega_0}$. In our numerical analysis we have chosen the first option. Finally, since it seems unrealistic to assume an increasing initial distribution at $Q_0^2 = 0.5 \text{ GeV}^2$, we, now, set $Q_0^2 = 0.8 \text{ GeV}^2$. Moreover we return to our initial convention and set $\varphi_{4S} = \varphi_{4A}$.

Fig. 17 shows the twist-four contributions at $Q^2 = 1 \text{ GeV}^2$ for the longitudinal and transverse photon. Compared to our first scenario, the twist-four corrections are, now, much larger. In order to understand this growth of the twist-four corrections we compare the first scenario presented in figs. 13a and 14a. Due to the increasing initial distribution, all four contributions are now larger than in the case of constant initial distributions. In particular, $\Delta F^{(2)}$ and $\Delta F^{(3)}$ are magnified by a similar factor, and the approximate cancellation works in the same way as before. For ΔF^R and ΔF^I , on the other hand, the approximate balance is distorted: at $Q^2 = 1 \text{ GeV}^2$ we are close to the initial scale, and ΔF^I is still small. Moreover, because of our choice of the $1/x$ -power ΔF^R has a stronger rise in $1/x$ than $\Delta F^{(2)}$ and $\Delta F^{(3)}$ and, therefore, dominates. As result, the twist-four corrections at $Q^2 = 1 \text{ GeV}^2$ are dominated by ΔF^R which is, now, much less balanced than in the previous scenario. By choosing in ΔF^R a weaker x -dependence at the initial scale and by setting our initial scale, as before, to $Q_0^2 = 0.5 \text{ GeV}^2$, it may be possible to partly restore the balance and to obtain a somewhat smaller twist-four correction. This scenario, therefore, represents a somewhat extreme possibility.

Nevertheless, the trend seen in this third scenario may be characteristic for increasing initial distributions. Initial parton distributions which increase at small x tend to increase the twist-four corrections at low Q^2 , in particular through ΔF^R . This pushes the balance between the positive ΔF^R and the negative ΔF^I into the positive direction, and, as in our case, may even lead to a net positive twist-four correction to the leading-twist structure function. If these tentative conclusions are correct, we have to interpret the scenario with rising initial conditions as being unrealistic. As discussed in the beginning of this paper, twist-four corrections could, in principle, provide an explanation for the observed change in the small x behavior at low Q^2 . In particular, with decreasing Q^2 , a negative transverse higher-twist could, because of its stronger rise at small x , overcome the $1/Q^2$ suppression and interfere with the rising leading-twist contribution. In this last scenario, however, we found that the opposite sign for transverse higher-twist is more likely, and leading- and higher-twist are adding up rather than compensating each other at low Q^2 . We believe that such a scenario is not very likely to be realistic.

5 Conclusions

In this paper we have made a first attempt to estimate twist-four corrections to the gluon structure function at small x and low Q^2 . We have collected all presently available analytic information on the twist-four gluon evolution equations and defined the terms which need to be included. Up to now DLA is the only approximation for which explicit expressions exist. One of the main features of gluonic twist-four corrections is the sign structure: we find, both in the transverse and in the longitudinal structure functions, terms with opposite signs which tend to compensate each other.

In the second part we have investigated how DIS diffractive dissociation (in particular the production of longitudinal vector mesons) can be used for constraining the free parameters, i.e. the initial conditions. As a main result, the AGK rules provide a bridge between DIS diffractive dissocia-

tion and the twist-four part of the four-gluon amplitude, but there remains a piece in the initial condition which cannot be determined in this way.

In our numerical part we have considered three different scenarios. For two of them we have chosen constant (in x) initial parton distributions at the input scale Q_0^2 , and we have varied the relative strength of pieces in the input distribution. In addition, we have studied also one scenario in which the input distribution rises in $1/x$. In general we find, both in the transverse and in the longitudinal structure functions, significant cancellations between terms with opposite signs which tend to weaken or even compensate each other. Moreover, the transverse twist-four corrections are larger than the longitudinal ones. For the scenarios with constant initial conditions the sum of the transverse twist-four corrections is negative, and at small x grows stronger than leading-twist. For $Q^2 = 1 \text{ GeV}^2$, $x = 10^{-4}$ twist-four ranges between 15% and 130% of leading-twist. Compared to the results of [4], our corrections seem to become significant in the right region. For the case of increasing initial conditions the different pieces of the transverse twist-four contributions add up to a positive higher-twist correction; we interpret this scenario as rather unrealistic. This may however change if one could go beyond the DLA. All our numerical results are based upon DLA accuracy and, therefore, should be taken as only “semiquantitative”.

Before firm conclusions can be drawn, several improvements have to be made. First of all, we need the complete LO calculations of the evolution kernels of the gluonic operators. Work along these lines is in progress [35], but it will take some time before one can start to perform numerical calculations. Secondly, as can be seen already from eqn. (2.38), the amount of computer work necessary to calculate the Q^2 evolution of the gluon operators is substantially larger than in the leading-twist case. Presently, it is not clear whether it is possible to find a closed expression also beyond DLA or whether we have to solve evolution equations in x -space. Attempts to solve the set of coupled evolution equations (2.18) will face difficulties with storage capacities. Finally, as discussed above, experimental information on specific final states is needed in order to restrict the arbitrariness in the choice of the initial conditions. In this first attempt we have used only the diffractive longitudinal vector meson production in order to obtain a first hint on the magnitude of twist-four. Besides this, other information of final states might be useful; a promising candidate might be a measurement of the two-particle correlation function as a function of rapidity [36].

Acknowledgements: One of us (J.B.) gratefully acknowledges the hospitality of the HEP Theory Division of Argonne National Laboratory and of the Theory Division of Fermilab where part of this work has been done. Discussions with R.K. Ellis have been very helpful and encouraging.

Appendix

We, first, give expressions for the vectors in color space $|i\rangle_\chi$ in the coupling scheme $\chi = (1234)$:

$$|1\rangle_{1234} = \frac{1}{8}\delta^{ab}\delta^{cd} \quad (\text{A.1})$$

$$|8_A\rangle_{1234} = \frac{-1}{6\sqrt{2}}f^{abl}f^{lcd} \quad (\text{A.2})$$

$$|8_S\rangle_{1234} = \frac{3}{10\sqrt{2}}d^{abl}d^{lcd} \quad (\text{A.3})$$

$$|10 + \bar{10}\rangle_{1234} = \frac{1}{2\sqrt{5}}\left\{\frac{1}{2}[\delta^{ad}\delta^{bc} - \delta^{ac}\delta^{bd}] + \frac{1}{3}f^{abl}f^{lcd}\right\} \quad (\text{A.4})$$

$$|27\rangle_{1234} = \frac{1}{3\sqrt{3}}\left\{\frac{1}{2}[\delta^{ad}\delta^{bc} + \delta^{ac}\delta^{bd}] - \frac{1}{8}\delta^{ab}\delta^{cd} - \frac{3}{5}d^{abl}d^{lcd}\right\}. \quad (\text{A.5})$$

They are normalized to one

$$\chi\langle i|j\rangle_\chi = \delta^{ij} \quad (\text{A.6})$$

and eigenstates of the BFKL color factor $t_{2\rightarrow 2}$:

$$(t_{2\rightarrow 2})_{\alpha\alpha'}|i\rangle_{\alpha\alpha'\beta\beta'} = \varepsilon_i|i\rangle_{\alpha\alpha'\beta\beta'} \quad (t_{2\rightarrow 2})_{\beta\beta'}|i\rangle_{\alpha\alpha'\beta\beta'} = \varepsilon_i|i\rangle_{\alpha\alpha'\beta\beta'}, \quad (\text{A.7})$$

where

$$(t_{2\rightarrow 2})_{12} = f^{aa'l}f^{lb'b} \quad (t_{2\rightarrow 2})_{13} = f^{aa'l}f^{lc'c} \quad \text{etc.} \quad (\text{A.8})$$

and $\varepsilon_i = \{-3, -\frac{3}{2}, -\frac{3}{2}, 0, 1\}$ for $i = \{1, 8_A, 8_S, 10 + \bar{10}, 27\}$. They are related to vectors in other coupling schemes via transitions with the matrices

$$\Lambda = \begin{pmatrix} \frac{1}{8} & -\frac{1}{2\sqrt{2}} & \frac{1}{2\sqrt{2}} & -\frac{\sqrt{5}}{4} & \frac{3\sqrt{3}}{8} \\ -\frac{1}{2\sqrt{2}} & \frac{1}{2} & -\frac{1}{2} & 0 & \frac{1}{2}\sqrt{\frac{3}{2}} \\ \frac{1}{2\sqrt{2}} & -\frac{1}{2} & -\frac{3}{10} & \sqrt{\frac{2}{5}} & \frac{3}{10}\sqrt{\frac{3}{2}} \\ -\frac{\sqrt{5}}{4} & 0 & \sqrt{\frac{2}{5}} & \frac{1}{2} & \frac{1}{4}\sqrt{\frac{3}{5}} \\ \frac{3\sqrt{3}}{8} & \frac{1}{2}\sqrt{\frac{3}{2}} & \frac{3}{10}\sqrt{\frac{3}{2}} & \frac{1}{4}\sqrt{\frac{3}{5}} & \frac{7}{40} \end{pmatrix} \quad \text{and} \quad P = \text{diag}(1, -1, 1, -1, 1) \quad (\text{A.9})$$

in the following way:

$$\begin{aligned} |i\rangle_{1234} &= \sum_j \Lambda_{ij} |j\rangle_{1324} & |i\rangle_{1324} &= \sum_j \Lambda_{ij} |j\rangle_{1234} \\ |i\rangle_{1234} &= \sum_j (P\Lambda P)_{ij} |j\rangle_{1423} & |i\rangle_{1423} &= \sum_j (P\Lambda P)_{ij} |j\rangle_{1234} \\ |i\rangle_{1324} &= \sum_j (P\Lambda)_{ij} |j\rangle_{1423} & |i\rangle_{1423} &= \sum_j (\Lambda P)_{ij} |j\rangle_{1324}. \end{aligned} \quad (\text{A.10})$$

Next, we give explicit expressions for the components of vector

$$\boldsymbol{\chi}(\omega\tilde{\nu}) \equiv \Sigma(\omega\tilde{\nu}) \mathbf{V} \quad (\text{A.11})$$

in eqns. (2.30) and (2.38). The results are the same for the three coupling schemes. Therefore, we list the components of $\boldsymbol{\chi}$ for the three contributing color states and write them as functionals of the auxiliary quantities $f_i(\omega\tilde{\nu})$, $i = 1 \dots 6$, and $g_j(\omega\tilde{\nu})$, $j = 1 \dots 7$. They are defined as follows:

$$\begin{aligned} f_1 &= -\frac{1}{32}\gamma_1 + \frac{3}{40}\gamma_8 - \frac{27}{160}\gamma_{27} - \frac{1}{4} & f_4 &= \frac{1}{\gamma_1} - \frac{1}{128}\gamma_1 - \frac{1}{16}\gamma_8 - \frac{27}{128}\gamma_{27} - \frac{1}{16} \\ f_2 &= -\frac{1}{128}\gamma_1 - \frac{1}{80}\gamma_8 - \frac{7}{640}\gamma_{27} - \frac{1}{16} & f_5 &= \frac{1}{\gamma_8} - \frac{1}{16}\gamma_1 - \frac{9}{200}\gamma_8 - \frac{27}{400}\gamma_{27} + \frac{3}{20} \\ f_3 &= -\frac{3}{32}\gamma_1 + \frac{9}{200}\gamma_8 - \frac{21}{800}\gamma_{27} - \frac{3}{20} & f_6 &= \frac{1}{\gamma_{27}} - \frac{27}{128}\gamma_1 - \frac{27}{400}\gamma_8 - \frac{49}{3200}\gamma_{27} - \frac{7}{80} \end{aligned} \quad (\text{A.12})$$

and

$$\begin{aligned} g_1 &= \frac{\sqrt{3}}{2}f_1 \cdot f_3 - 3\sqrt{3}f_2 \cdot f_5 & g_4 &= f_5 \cdot f_6 - \frac{3}{2}f_3^2 \\ g_2 &= \frac{9\sqrt{2}}{2}f_2 \cdot f_3 - \frac{\sqrt{2}}{2}f_1 \cdot f_6 & g_5 &= f_4 \cdot f_6 - 27f_2^2 \end{aligned} \quad (\text{A.13})$$

$$\begin{aligned} g_3 &= \frac{3\sqrt{6}}{2}f_1 \cdot f_2 - \frac{\sqrt{6}}{2}f_3 \cdot f_4 & g_6 &= f_4 \cdot f_5 - \frac{1}{2}f_1^2 \\ g_7 &= 9f_1 \cdot f_2 \cdot f_3 + f_4 \cdot f_5 \cdot f_6 - \frac{1}{2}f_1^2 \cdot f_6 - 27f_2^2 \cdot f_5 - \frac{3}{2}f_3^2 \cdot f_4, \end{aligned} \quad (\text{A.14})$$

where the functions $\gamma_i(\omega\tilde{\nu})$ are the diagonal elements of matrix $\gamma(\omega\tilde{\nu})$ in eqn. (2.28), and we have used γ_8 instead of γ_{8_S} . With these functions the elements of the vector $\boldsymbol{\chi}$ are given by the following expression:

$$g_7 \cdot \chi_j = v_j g_7 \gamma_j + \sum_{i=1}^6 g_i \left(\kappa_{1i}^{(j)} \gamma_j \gamma_1 + \kappa_{2i}^{(j)} \gamma_j \gamma_8 + \kappa_{3i}^{(j)} \gamma_j \gamma_{27} + \kappa_{4i}^{(j)} \gamma_1 + \kappa_{5i}^{(j)} \gamma_8 + \kappa_{6i}^{(j)} \gamma_{27} \right), \quad (\text{A.15})$$

where $j \in \{1, 8_S, 27\}$, $v_1 = 2$, $v_8 = 4\sqrt{2}$, $v_{27} = 6\sqrt{3}$ (cf. (2.29)) and the coefficients $\kappa_{li}^{(j)}$ are listed in table 5. The pole at $\omega\tilde{\nu} = 4(1 + \delta)N_c \alpha_s / \pi$ (eqn. (2.39)) is due to a zero of function g_7 , eqn. (A.14).

Finally, the color tensor d^{abcd} in (2.41) has the form [9]:

$$\begin{aligned} d^{abcd} &= \text{tr}\{t^a t^b t^c t^d\} + \text{tr}\{t^d t^c t^b t^a\} = \\ &= \frac{1}{6}\delta^{ab}\delta^{cd} + \frac{1}{4}d^{abl}d^{lcd} - \frac{1}{4}f^{abl}f^{lcd} \\ &= \frac{1}{6}\delta^{ad}\delta^{bc} + \frac{1}{4}d^{adl}d^{lbc} + \frac{1}{4}f^{adl}f^{lbc}, \end{aligned} \quad (\text{A.16})$$

where the Gell-Mann matrices t^a are normalized to

$$\text{tr}\{t^a t^b\} = \frac{1}{2}\delta^{ab}. \quad (\text{A.17})$$

References

- [1] M.Glück, E.Reya, A.Vogt, *Z.Phys.* **C 67** (1995) 433, *Eur.Phys.J.* **C 5** (1998) 461.
- [2] A.D.Martin, R.G.Roberts, W.J.Stirling, *Phys.Lett.* **B 387** (1996) 419.
- [3] R.Ball, S.Forte, *Nucl.Phys.Proceedings Suppl.* **54 A** (1997) 163.
- [4] ZEUS Collaboration, J.Breitweg et. al., *Eur.Phys.J.* **C 7** (1999) 609.
- [5] R.K.Ellis, F.Hautmann, B.R.Webber, *Phys.Lett.* **B 48** (1995) 582; R.K.Ellis, Z.Kunszt, E.M.Levin, *Nucl.Phys.* **B 420** (1994) 517; ERRATUM-ibid. **B 433** (1995) 498.
- [6] A.B.Bukhvostov, G.V.Frolov, L.N.Lipatov, E.A.Kuraev, *Nucl.Phys.* **B 258** (1985) 601.
- [7] R.K.Ellis, W.Furmanski, R.Petronzio, *Nucl.Phys.* **B 212** (1983) 29.
- [8] E.A.Kuraev, L.N.Lipatov, V.S.Fadin, *Sov.Phys.JETP* **44** (1976) 443, ibid. **45** (1977) 199, Ya.Ya.Balitskii, L.N.Lipatov, *Sov.J.Nucl.Phys.* **28** (1978) 822.
- [9] J.Bartels and M.Wüsthoff, *Z.Phys.* **C 66** (1995) 157.
- [10] M.G.Ryskin, *Z.Phys.* **C 57** (1993) 89.
- [11] S.J.Brodsky, L.Frankfurt, J.F.Gunion, A.H.Mueller, and M.Strikman, *Phys.Rev.* **D 50** (1994) 3134.
- [12] J.C.Collins, L.Frankfurt, M.Strikman, *Phys.Rev.* **D 56** (1997) 2982.
- [13] A.D.Martin, M.G.Ryskin, T.Teubner, *Phys.Rev.* **D 55** (1997) 4329, ibid. **D 56** (1997) 3007.
- [14] V.A.Abramovsky, V.N.Gribov, O.V.Kancheli, *Sov.J.Nucl.Physics* **18** (1974) 308.
- [15] S.Gottlieb, *Nucl.Phys.* **B 139** (1978) 125, M.Okawa, *Nucl.Phys.* **B 172** (1980) 481, ibid. **B 187** (1981) 71, S.P.Luttrell, S.Wada, B.R.Webber, *Nucl.Phys.* **B 188** (1981) 219, R.L.Jaffe, M.Soldate, *Phys.Rev.* **D 26** (1982) 49, R.L.Jaffe, *Nucl.Phys.* **B 229** (1983) 205, J.Qiu, *Phys.Rev.* **D 42** (1990) 30.
- [16] J.Bartels, *Phys.Lett.* **B 298** (1993) 204, *Z.Phys.* **C 60** (1993) 471.
- [17] V.S.Fadin, L.N.Lipatov, *Phys.Lett.* **B 429** (1998) 127.
- [18] M.Wüsthoff, PhD Thesis, University of Hamburg 1995, DESY-95-166.
- [19] L.D.Faddeev, *Sov.Phys.JETP* **12** (1961) 1014.
- [20] E.M.Levin, M.G.Ryskin, A.G.Shuvaev, *Nucl.Phys.* **B 387** (1992) 589.
- [21] J.Bartels, M.G.Ryskin, *Z.Phys.* **C 62** (1994) 425.
- [22] G.P.Salam, *J.High Energy Phys.*, 07(1998)019.
- [23] A.De Rujula et al., *Phys.Rev.* **D 10** (1974) 1649.
- [24] R.Ball, S.Forte, *Phys.Lett.* **B 335** (1994) 77, *Phys.Lett.* **B 336** (1994) 77.
- [25] J.Bartels, H.Lotter, M.Wüsthoff, *Phys.Lett.* **B 379** (1996) 239; ERRATUM-ibid. **B 382** (1996) 449.
- [26] N.N.Nikolaev, B.G.Zakharov, *Phys.Lett.* **B 332** (1994) 177.
- [27] J.Bartels, M.Wüsthoff, *Proc. DIS97*, Chicago 1997.
- [28] J.Bartels, M.Strikman, in preparation.

- [29] J.Bartels, H.Jung, M.Wüsthoff, DESY-99-027, hep-ph/99 03 265.
- [30] M.G.Ryskin, M.Besancon, *Proc. Physics at HERA*, Hamburg, Oct.1991 (eds. W.Buchmüller and G.Ingelman) **Vol. 1**, p. 215.
- [31] E.Levin, M.Wüsthoff, *Phys.Rev.* **D 50** (1994) 4306.
- [32] J.Bartels, M.G.Ryskin, *Z.Phys.* **C 76** (1997) 241.
- [33] A.D.Martin, R.G.Roberts, M.G.Ryskin, W.J.Stirling, *Eur.Phys.J.* **C 2** (1998) 287.
- [34] J.N.Lyness, T.J.Kaper, *SIAM J.Sci.Stat.Comput.* **8** (1987) 1005.
- [35] J.Bartels, C.Bontus, H.Spiesberger, work in progress.
- [36] K.Charchula, E.M.Levin, *Proc. Physics at HERA*, Hamburg, Oct.1991 (eds. W.Buchmüller and G.Ingelman) **Vol. 1**, p. 223.

i	1	2	3	4	5	6
$\kappa_{1i}^{(1)}$	$\frac{3\sqrt{3}}{32}$	$\frac{\sqrt{2}}{16}$	$\frac{3\sqrt{6}}{16}$	$\frac{1}{64}$	$\frac{1}{8}$	$\frac{27}{64}$
$\kappa_{2i}^{(1)}$	$\frac{9\sqrt{3}}{20}$	$\frac{7\sqrt{2}}{40}$	$-\frac{3\sqrt{6}}{40}$	$\frac{1}{8}$	$-\frac{3}{10}$	$\frac{27}{40}$
$\kappa_{3i}^{(1)}$	$\frac{213\sqrt{3}}{160}$	$\frac{81\sqrt{2}}{80}$	$\frac{51\sqrt{6}}{80}$	$\frac{27}{64}$	$\frac{27}{40}$	$\frac{189}{320}$
$\kappa_{4i}^{(1)}$	$\frac{3\sqrt{3}}{4}$	$\frac{\sqrt{2}}{2}$		$\frac{1}{4}$		
$\kappa_{5i}^{(1)}$	$\frac{6\sqrt{3}}{5}$	$-\frac{6\sqrt{2}}{5}$		2		
$\kappa_{6i}^{(1)}$	$\frac{21\sqrt{3}}{20}$	$\frac{27\sqrt{2}}{10}$		$\frac{27}{4}$		
$\kappa_{1i}^{(8)}$	$\frac{9\sqrt{6}}{80}$	$\frac{7}{80}$	$-\frac{3\sqrt{3}}{80}$	$\frac{\sqrt{2}}{32}$	$-\frac{3\sqrt{2}}{40}$	$\frac{27\sqrt{2}}{160}$
$\kappa_{2i}^{(8)}$	$\frac{3\sqrt{6}}{10}$	$-\frac{3}{5}$	$-\frac{9\sqrt{3}}{25}$	$\frac{\sqrt{2}}{4}$	$\frac{9\sqrt{2}}{50}$	$\frac{27\sqrt{2}}{100}$
$\kappa_{3i}^{(8)}$	$\frac{51\sqrt{6}}{80}$	$-\frac{27}{80}$	$\frac{99\sqrt{3}}{400}$	$\frac{27\sqrt{2}}{32}$	$-\frac{81\sqrt{2}}{200}$	$\frac{189\sqrt{2}}{800}$
$\kappa_{4i}^{(8)}$		$\frac{1}{4}$	$\frac{3\sqrt{3}}{4}$		$\frac{\sqrt{2}}{2}$	
$\kappa_{5i}^{(8)}$		2	$\frac{6\sqrt{3}}{5}$		$-\frac{6\sqrt{2}}{5}$	
$\kappa_{6i}^{(8)}$		$\frac{27}{4}$	$\frac{21\sqrt{3}}{20}$		$\frac{27\sqrt{2}}{10}$	
$\kappa_{1i}^{(27)}$	$\frac{71}{160}$	$\frac{9\sqrt{6}}{80}$	$\frac{17\sqrt{2}}{80}$	$\frac{3\sqrt{3}}{64}$	$\frac{3\sqrt{3}}{40}$	$\frac{21\sqrt{3}}{320}$
$\kappa_{2i}^{(27)}$	$\frac{17}{20}$	$-\frac{3\sqrt{6}}{40}$	$\frac{33\sqrt{2}}{200}$	$\frac{3\sqrt{3}}{8}$	$-\frac{9\sqrt{3}}{50}$	$\frac{21\sqrt{3}}{200}$
$\kappa_{3i}^{(27)}$	$\frac{189}{160}$	$\frac{81\sqrt{6}}{80}$	$\frac{189\sqrt{2}}{400}$	$\frac{81\sqrt{3}}{64}$	$\frac{81\sqrt{3}}{200}$	$\frac{147\sqrt{3}}{1600}$
$\kappa_{4i}^{(27)}$	$\frac{1}{4}$		$\frac{\sqrt{2}}{2}$			$\frac{3\sqrt{3}}{4}$
$\kappa_{5i}^{(27)}$	2		$-\frac{6\sqrt{2}}{5}$			$\frac{6\sqrt{3}}{5}$
$\kappa_{6i}^{(27)}$	$\frac{27}{4}$		$\frac{27\sqrt{2}}{10}$			$\frac{21\sqrt{3}}{20}$

TABLE 5: Expansion coefficients for the three different color states in eqn. (A.15).